No mantle convection but efficient tidal forces move plates (Corrected)

Lubor Ostřihanský

Nad Palatou 7,150 00 Prague 5 – Smíchov, Czech Republic.

ostrih@tiscali.cz

Abstract.

First part of the paper deals with obscure imagination of mantle convection, which contradicts to any real observations. Geological maps clearly show plates rotation round South Pole and the opening of back-arc basins confirms plates westward movements. Common action of equator-fleeing force and tidal friction facilitates the plate movement westward and northward. Hotspots confirm plate movements and triple junction mantle convection excludes. Calculated north-south tidal torques and tidal friction torques state when earthquakes by tides can be triggered. Plate movement and earthquakes triggering are bound to the space released by subduction. Not all Full or New Moons are favorable for earthquake triggering; discarding can be caused by low tidal torques or Moon and Sun torques acting oppositely. For Earth's rotation variations and for the plate movement the nodal Moon 18.61 years periodicity, sidereal Moon 27.56 days periodicity and their semidiurnal variations are important for earthquake triggering and earthquakes prediction.

Introduction

Even already Alfred Wegener (1929) considered tides as drivers for continents. Nevertheless plate tectonics occurring in sixties and seventies of 20th century glorified mantle convection as plate driver. In 1931 Arthur Holmes introduced the concept of mantle convection as a motive force to drive continental drift. Harry Hess (1962) adopted the idea of mantle convection as a critical component of seafloor spreading, which became an integral part of plate tectonics. Despite 50 years of intense scientific investigations, there is yet no unambiguous evidence that mantle convection actually exists. On the other hand the detailed and convincing study was presented by Schubert et al. (2004), freely available on Internet with 940 pages breaking any doubts, which could occurred against mantle convection. In spite of this, many studies occur confirming tidal plate driving mechanism or tidal earthquakes triggering: (Bostrom, 1971; Nelson and Temple, 1972; Moore, 1973; Ostřihanský, 1978, 1997; Doglioni, 1990, 1994). Many papers occur in 21st century (Ostřihanský, 2004, 2012a,b, 2015, 2019b), (Doglioni et al., 2003, 2005, 2007, 2011), (Metevier et al., 2009); (Tanaka, 2010, 2012); (Varga and Grafarend, 2018); (Riguzzi et al., 2010). Let us mention that papers of Bostrom (1971 and 1973) consider mantle convection as induced by tides. Doglioni (1990 and next till 2011) considers mantle convection, but influenced by tidal drag and similarly Riguzzi et al. (2010). The purpose of this paper is to show that the mantle convection is an absolute nonsense and no mantle convection, but conduction by its slow movement has dominant effect on plate tectonics with tides moving plates and triggering earthquakes. Conclusions stem from the last author paper of Ostřihanský (2020) emphasizing dominant action of tides on Earth's rotation variations and confirming the plate movement driven by tides from geodetic measurements by geodetic techniques of Global Navigation

Satellite System (GNSS), analyzing by Fast Fourier Transform tidal periods in the plate movement (Zaccagnino et al., 2020).

There are some doubts about effect of tidal waves on plates. The effect of Mf declinational zonal wave is significantly larger than the impact of the Mm elliptic one and also input of solar Ssa declinational wave has a more or less similar magnitude. Sectorial semi-diurnal waves are not variants of zonal waves and have no effect on the rotation of the Earth, as far as the earth tides are considered. Tides play a significant role in changes in length of day (LOD), but their impact is not dominant. Oceanic and especially atmospheric angular momentums are more significant.

To answer this objection, tidal forces acting on lithospheric plates are calculated on Appendix (Calculations of tidal forces). This paragraph presents formulas calculating tidal forces for given parameters of Moon and Sun positions. It is true that globally angular momentum fluctuations of the atmosphere and changes in the length of the day (Hide 1984) have very similar graph. However just details of LOD graph present in many cases the tool to proof the earthquakes tidal origin.

Geologic constraints

Geological World Atlas (Heezen and Tharp 1985) presents evident westward movements of lithospheric plates (Fig. 1). Antarctic Ocean shows an exact whole westward lithosphere rotation around the South Pole, by the curvature of Scotia Sea basin. Therefore no tectonic equator of Doglioni (1990), but exact lithosphere rotation rounds the pole. Caribbean plate, situated at 15º latitude, keeps similarly westward lithosphere movement. Latitudinal mid-ocean ridges intruding deeply to polar region

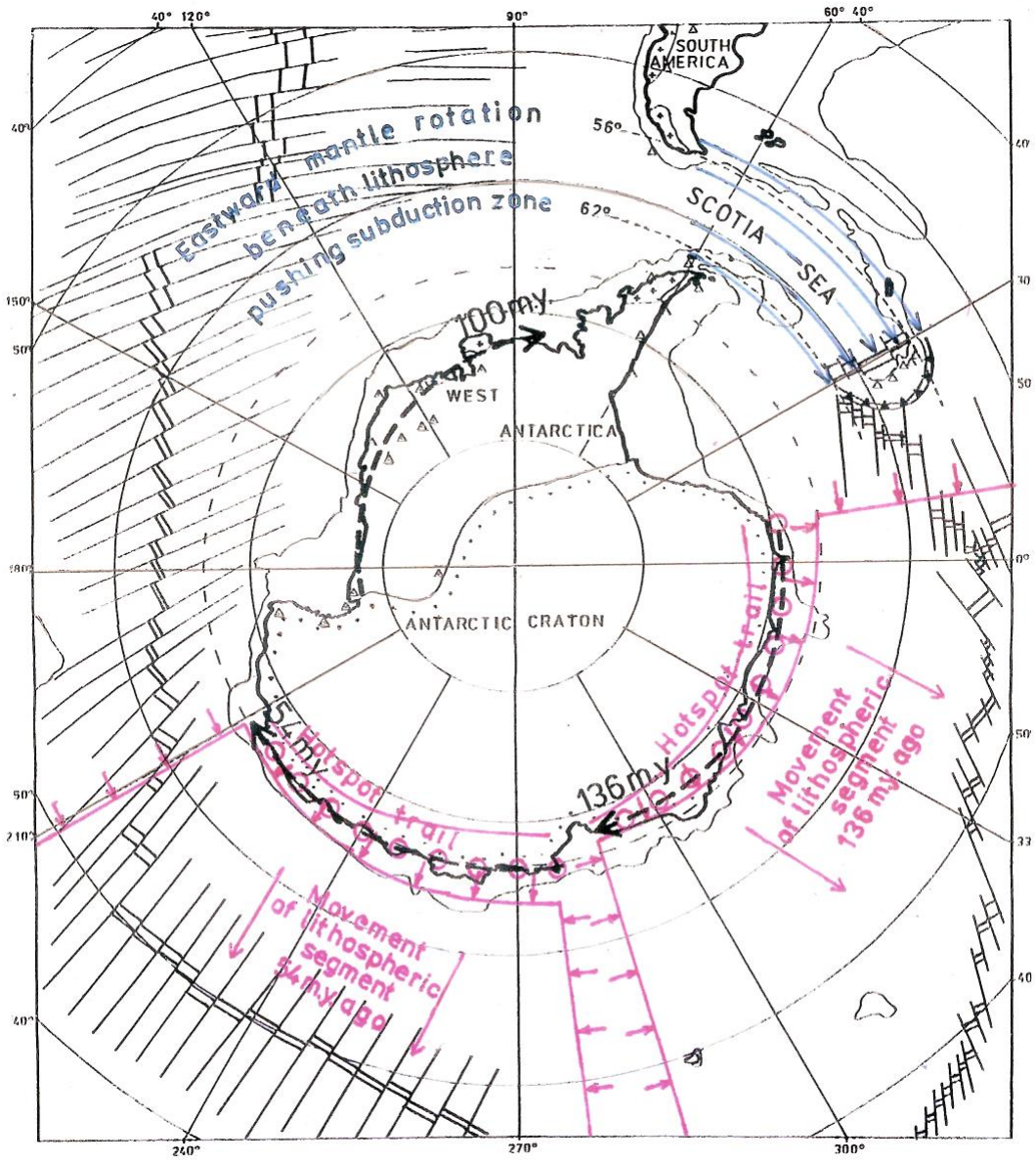

Figure 1. Rotational and equator-ward movements in Antarctica. (Ostřihanský 1997). (The mid-ocean ridge position according to Heezen and Tharp (1985)).

created favorable conditions for the movement of released segments separated from remaining parts of Antarctica by equator-fleeing force 130, 100 and 54 M.Y. ago. The Scotia Sea basin situated exactly between 56º and 62º latitudes represents the most convincing phenomenon of whole lithosphere rotation round the pole.

There are some differences in movement of north and south hemispheres. The movement of the Eurasian and North American plates demonstrates the westward movement of northern hemisphere. The movement of Eurasian plate is documented by opening of back-arc basins on its eastern side, where subducting oceanic lithosphere of the Pacific plate is firmly mantle anchored in Kuril Trench, Japan trench, Nankai Trench, Ryukyu Trench, and Philippine trench. Eurasian plate receding westward opens behind itself oceanic lithosphere of these basins. Slow differences in westward movements of Eurasian and North American plates is evident on narrow opening of the Atlantic ocean, but quick movement of both plates is evident from overriding of the East pacific Rise.

Movement of Southern hemisphere starts with South Fiji Basin separated from Tonga trench. The Indo-Australian plate moves mostly northward and its movement westward between Africa is unexpressive, separated by Indian ridge. Africa moves westward slightly quicker, but southern part of Atlantic Ocean opens widely. Resulting movement of the Southern hemisphere is slower, not crossing the East Pacific Rise.

Dominant movements on the Earth are the northward movements, evoked by north-south tidal torques, calculations of these torques are presented in Appendix. Owing to obliquity of Earth rotation axis, tides drift out of equator all continental and oceanic plates. Not Wegener’s Polfluchtkraft but ëquator-flucht (equator-fleeing force) is dominant force driving plates. Diurnal and Moon’s sidereal (27.56 days) variations together with Moon nodal (18.61 years) are dominant variations driving plates, either northward, because at present time subduction is possible only on northern hemisphere and facilitate westward movement by mechanism overcoming

friction of weak tidal friction torque10^{16} Nm by perpendicular variations of ëquator-flucht 10^{22} Nm (Fig. 2). (Similarity with **drilling by pneumatic hammer** pushig the drill by weak hand). Torqueses in this paper are given in Nm (Newton.metter). 1 Nm=1 J (Joule), what reperesents energy.

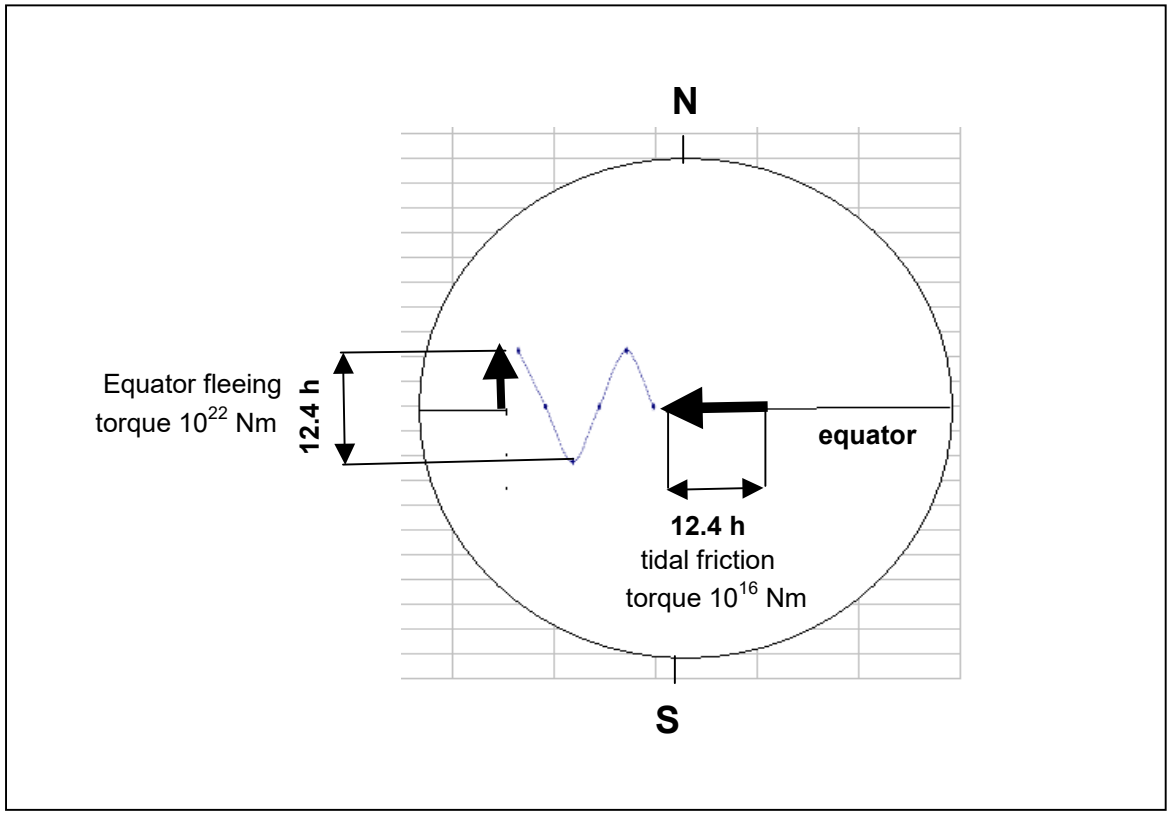

Figure 2. The whole lithosphere is subjected to two perpendicularly acting forces: tidal friction 10^{16} Nm and equator-fleeing north directing 10^{22} Nm. By permanent action of these forces acting in 12.4 h period (Moon 12.42 h, Sun 12 h) the whole lithosphere moves westward. (Half value of equator-fleeing force concerns plates moving northward, because southern component is damped in mid-ocean ridge, which acts as ratcheting mechanism). Numbers on periodic curve of figure are maximum and minimum stresses acting on equatorial lithosphere calculated from equation (2) of Appendix with periodic addition or subtraction of

stress of Sun (eqution 1). On lithosphere act both forces, zonal equator flying and westward drift which decelerates the Earth (Lambeck, 1977).

Plates move only northward, because after the decay of Gondwana, the oldest and heaviest oceanic litgosphere remained along southerm rim of Laurasia, prone to subduct by gravity descent.

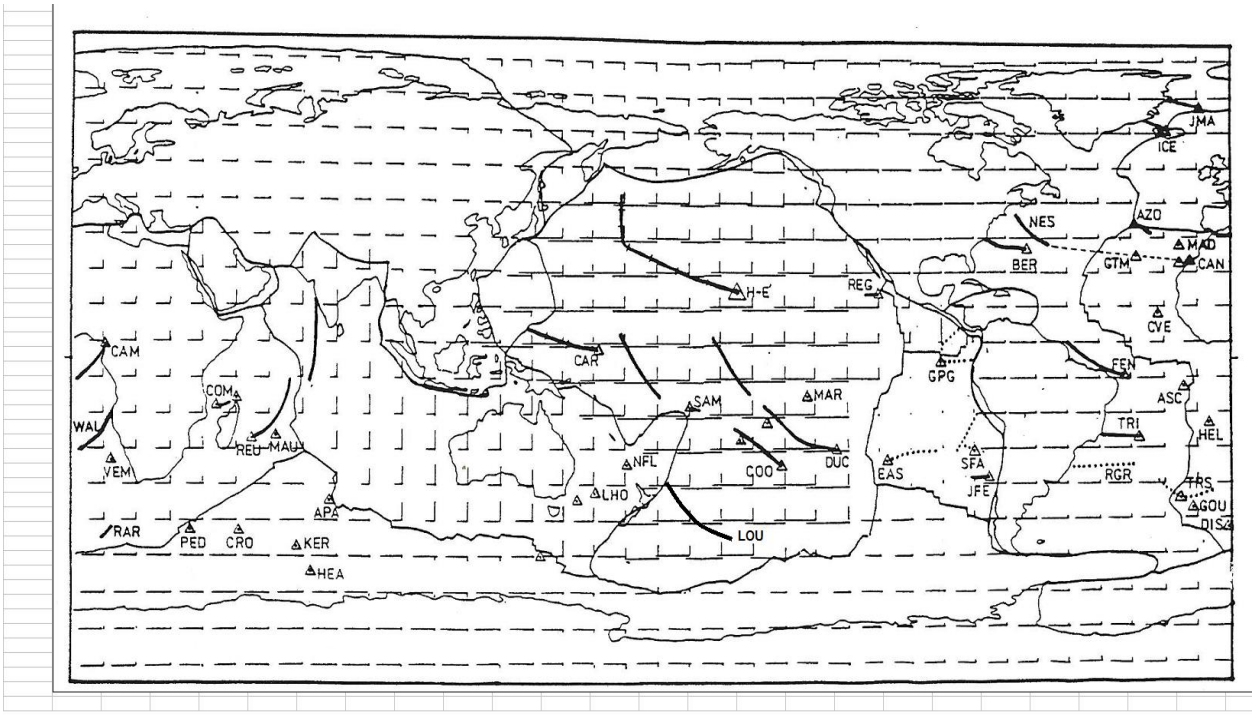

Figure 3a. Minster and Jordan (1978) established imagination of no rotation frame, according which lithospheric plates moved chaotically against each other or dispersed in mid-ocean ridges supporting imagination of mantle convection. Because small plates as Nazca and Cocos remain stable on mantle then calculation shows that plates move in direction of westward and northward components as depict on figure. Solid curves depict hotspot tracks, which show that originally plates moved northward (Reunion hotspot (REU), disrupted by mid-ocean ridge. Original movement of Hawaii-Emperor Seamount Chain (H-R) has been also northward but later prevailed westward component. New England Seamount (NES)

shows interruption of hotspot track by Mid-Atlantic Ridge and hotspot stable position in Canary Island (CAN), (Ostřihanský, 1997).

It is necessary to realize an absolute nonsense of mantle convection hypothesis, which introduce so called two layered mantle convection in upper and lower mantle, to distinguish convection in small back-arc basins and in the whole large plate movement. Supporters of mantle convection established no net rotation frame, apparently chaotic movement of plates (Minster and Jordan 1978). How simply plates move by tides shows Fig. 3a (Ostřihanský 1997).

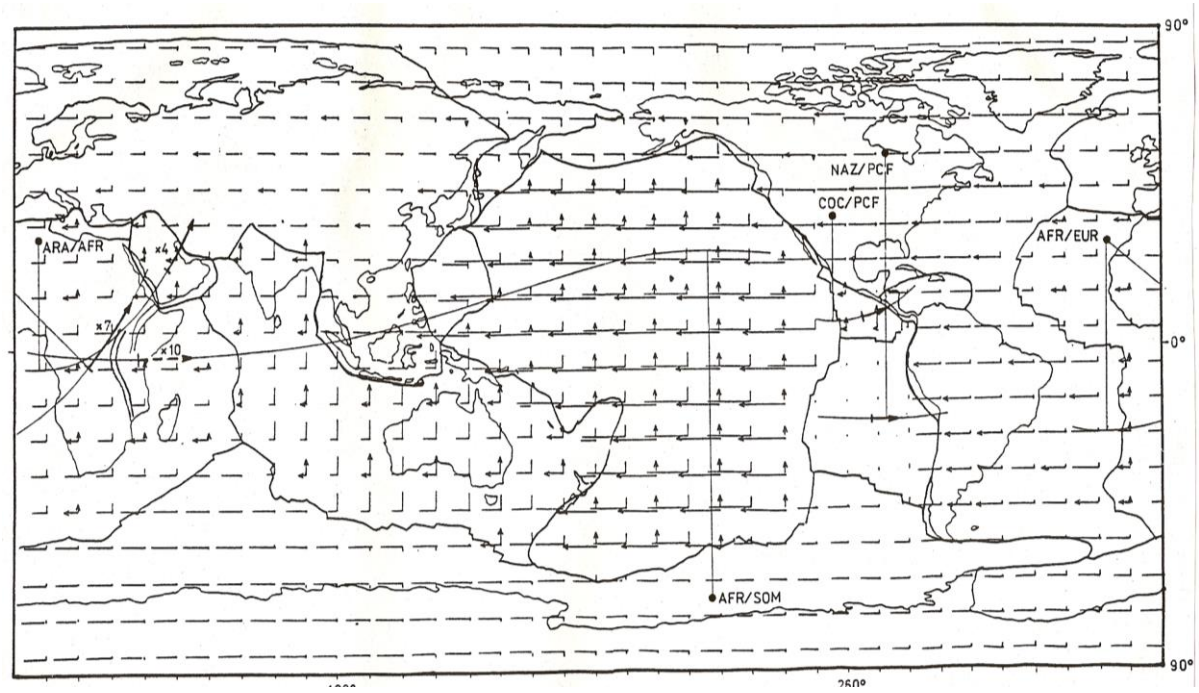

Figure 3b.This figure depicts components of the plate movement with arrows. Points mark Euler's poles, what in previous studies was recommended to find origin of the plate movement (Ostřihanský, 1997).

Mantle convection contradicts to any real imaginations. Arguments presented in first 7 columns of the paper try to confirm this statement. The next column "Acttion of tides on Earth" present tides as dominant force moving plates.

Continental fragments in oceanic lithosphere

Microcontinents remaining behind moving oceanic lithosphere cannot be explained by mantle convection. Mid-ocean ridge producing magma by convection cannot create continental fragments, however mid–ocean ridges are opened by tides in faults by the movement of plates. Mid-ocean ridge can be created anywhere on rear side of continent or mid-ocean ridges extinct and new closer to continent are created. Seychelles is a continental fragment separated from Indian continent (Vink et al., 1984), Kerguelen Plateau, lost behind movement of India, situated in middle of Indian Ocean, is the best example of it. (Houtz et al., 1977) and many others in Broek and Gaina (2020). Mid-ocean ridges and transform faults form an orthogonal system with often series of running ridges e.g. in East Pacific Rise. This phenomenon is considered by Schubert et al., (2004, page 29) as unclear for mantle convection. Fig. 4b shows construction of direction of transform faults in SW Indian Ocean ridge by subtraction of speeds of adjacent plates. This confirms that mid-ocean ridges are surface features and not deep structures of mantle convection.

Hotspots and their tracks

Hotspots and their tracks present unsolvable problem of mantle convection. Hotspots are simple strikes of oceanic lithosphere by meteorites. Strikes in continental

lithosphere are improbable unless continent overrides oceanic lithosphere with hotspot. This can cause catastrophic eruption (Yellowstone). Mid-ocean ridges override hotspots, which they then remain by uplift in new plate. Very large meteorite can cause strike even through continent. Example: Baffin Bay, then movement eastward under westward moving lithosphere beneath Greenland as far as Iceland with uplift. Even this hotspot has a shallow depth (Foulger et al., 2001). Hotspot tracks mark the plate movement. The primary cause of the plate movement is formation of subduction zone, then the push from tidal force, as it will be explain in next. Originally the Pacific plate moved only northward. Formation of new subducton zone on NW caused the movement in this direction. Hawaii-Emperor Seamount Chain is the proof of it (H-E Fig. 3a). Reunion hotspot with Deccan Traps shows interruption of hotspot direction northward as the Indo-Australian plate proves (REU Fig. 3a). Louiswill ridge in South Pacific (LOU) shows bending but not so sharp as Hawaii-Emperor Seamount. New England Ridge in northern Atlantic (NES) is a hotspot tack interrupted by Atlantic mid-ocean ridge, which started in Cap Verde, now fixed in African plate.(Hotspot tracks see in Fig. 3a). Mantle plumes are unrealistic imagination originating in core-mantle boundary to support their fixed position in mantle considering mantle convection.

Only impact of meteorites can create point sources of ascending magma for hotspots. . First, hotspots are firmly fixed in mantle and therefore hotspot tracks direct in opposite direction from mid-ocean ridge. In case of mantle convection hotspot tracks would direct towards mid-ocean ridge. Mantle forms a firm and solid carapace around liquid core. Ascent any hot mantle plumes is impossible unless any cracks occur in mantle bottom facilitating the plume ascent. These ascents never can be a point sources, as in reality are, but linear or curvilinear features on Earth’s surface.

Mantle plimes are point sources of different size produced by meteoric impact protruding oceanic lithosphere; otherwise meteor can splinter on continental lithosphere. Meteoritic mantle plume is heated by surrounding hot mantle but inside is melted because its solid consistence prevent any action of pressure increasing according to Clausius Clappeyron equation melting point and light component uprise and heavy component descends. Similar effect is evident in subdction. Solid descending oceanic lithosphere is not affected by the increase of pressure but heated by surrounding environment (**effect of bathyscaphe** produced from strong steel). Cracks occur on both sides of subduction zone but melted part is inside. Light material uprise forming island arc volcanics and heavy part descends and burns a hole in mantle. It is really hardly to imagine how againat upword streaming magma of back-arc basin volcanics mantle convection drive oceanic lithosphere down ward.

Simple explanation of westward movement follows from Eartth's deceleration caused by tidal friction (Lambeck 1977) and Fig. 1 confirms almost exact westward movement of American and Eurasian plates. Other plates have components of northward and southward movements depicted on Figs 3ab.

Triple junctions phenomena exclude mantle convection

Triple junctions of three mid-ocean ridges exclude existence of convection in the mantle. Supposing mantle convection, then every mid-ocean ridge has two convection currants bilaterally acting to both sides of the mid-ocean ridge pushing plates apart. If three mid-ocean ridges intersect in one point, then convection

currents from adjacent mid-ocean ridges join in one stream directing from point of intersection. Created streams rupture mid-ocean ridges apart and finish the triple junction existence.

Let us demonstrate formation of Rodriguez triple junction in Indian Ocean (Fig. 4a): Considering the Antarctic plate as stable on the South Pole, then the Southeast and Southwest Indian Ocean ridges move with ½ speed of the Indo Australian and African plates and the directions of fractures crossing the mid-ocean ridge is given by vectorial subtraction of adjacent plates (on Fig. 4b marked by red lines).

Fig. 4b shows that every plate has its own movement given by forces that act on it and not by a speculative traction of convection cell below it. In case of convection, fractures intersecting the mid-ocean ridges were trajectories of the plate movement. Because this is not the case and fractures intersecting mid-ocean ridges are resultants of the movements of adjacent plates, this result definitely discards any imagination of the mantle convection driving plates.

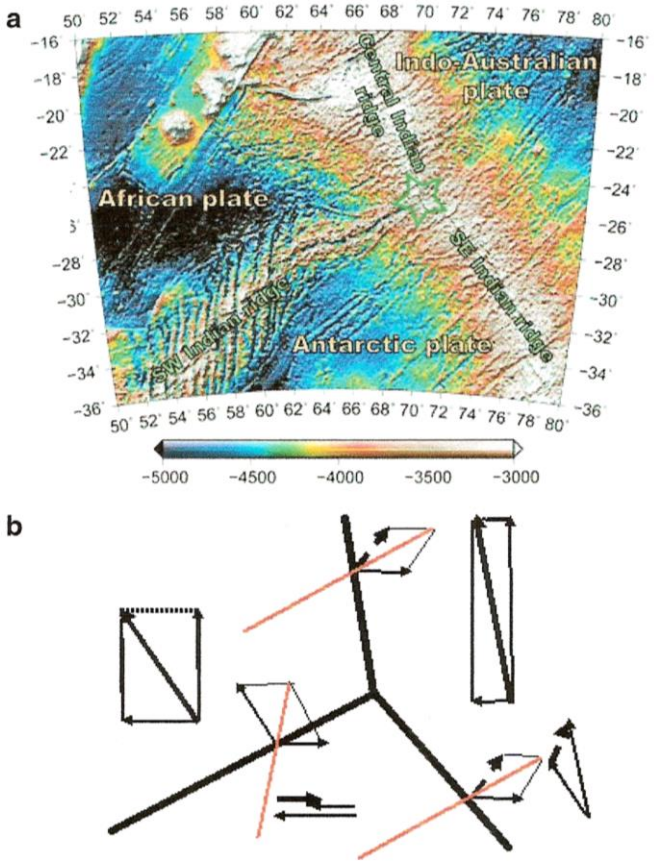

247

248

249 **Fig. 4a.** Rodriguez triple junction in the Indian Ocean separating African, Indo-Australian and
250 Antarctic plates by SW Indian, SE Indian and Central Indian Ocean ridges. Considering
251 fractures intersecting mid-ocean ridges as trajectories of the plate movement then e.g. the
252 African plate has paradoxically two Euler's poles of the plate rotation.
253 **Fig. 4b.** gives explanation. Every plate has two components of its movement: the westward
254 and northward. The African plate moves westward and northward, the Indo-Australian plate
255 moves less distinctively westward but strongly northward. The Antarctic plate has no
256 northward components because is firmly fixed on the South Pole. It moves only eastward by
257 difference between westward components of African end Indo Australian plates. Because the
258 Antarctic plate has no northward components the SW Indian and SE Indian Ocean ridges
259 move with ½ speed of African and Indo-Australian plates. The directions of fractures

intersecting mid-ocean ridges (marked by red lines) are resultant of ½ plate speed and vectorial difference speed of adjacent plates.

Action of tidal forces gives an excellent explanation of Himalayas mountain belt formation

In 2012 van Hinsbergen et al. presented detailed description of India and Asia collision. Following their paleomagnetic data acquisition, it is possible to describe action of tides driving plates, their movement and collision. In late Triassic Gondwana separated from Laurasia by equator-fleeing tidal force 10^{22} Nm, using ratcheting mechanism preventing movement northward, but subducting old oceanic lithosphere in front of Gondwana on south facilitated the movement southward, pushing Gondwana far south over south pole. Witness of that movement is Transantarctic Mountain Range and mid-ocean ridge situated in middle of ocean between Gondwana and Laurasia, which remained as fossil ridge. In mantle convection hypothesis mid-ocean ridges have fixed position in mantle. However tidal forces cause that mid-ocean ridges move and mid–ocean ridge, which moved with 1/2 speed of Gondwana remained as fossil ridge in Neotethys Ocean, in van Hinsbergen et al. (2012) called later as Tibetan Himalayan microcontinent.

140 Ma ago large oceanic plate has been created comprising Neotectonic Ocean as far as subduction zone in font of Asia and with small continent Greater India on rear side. This part has been torn off Gondwana by tidal force because this plate exceeded far equator and subducting oceanic lithosphere in front of this plate made this movement northward possible and caused consumption of Neotethys oceanic lithosphere and formation of forarc volcanics in Lhasa. 50 Ma continuing subduction

created collision of fossile mid-ocean ridge later called Tibetan Himalayas containing ophiolites as representants of former mid-ocean volcanics. These volcanics can never subduct because are too light and always form obduction. (See similar form of obduction in Taiwan, Fig. 6). 23 Ma shows final hard collision of Indian lithosphere and subducting of oceanic lithosphere of Greater Indian Basin forming the main central thrust in front of South Tibetan detachment.

Mantle convection absolutely incorrect explains origin of marginal basins

If the adjacent continent is being driven up against the trench, as in Chile, marginal basins do not develop. If the adjacent continent is stationary relative to the trench, as in the Marianas, the foundering of the lithosphere leads to a series of marginal basins as the trench migrates seaward.(Shubert et al. 2004, page 39). These authors do not realize that lithosphere moves westward by tides. The mechanism is following (Fig. 5): Old oceanic lithosphere drops down to mantle by gravity (Model 1), but if continental lithosphere moves westward, creates back-rcbasin with mid-ocean ridge in middle (Model 2). If continental lithosphere moves westward in front of suvducting oceanic lithosphere (Model 3), continent overrides it, liquidate it without regard of age and can also override even mid-ocean ridge.

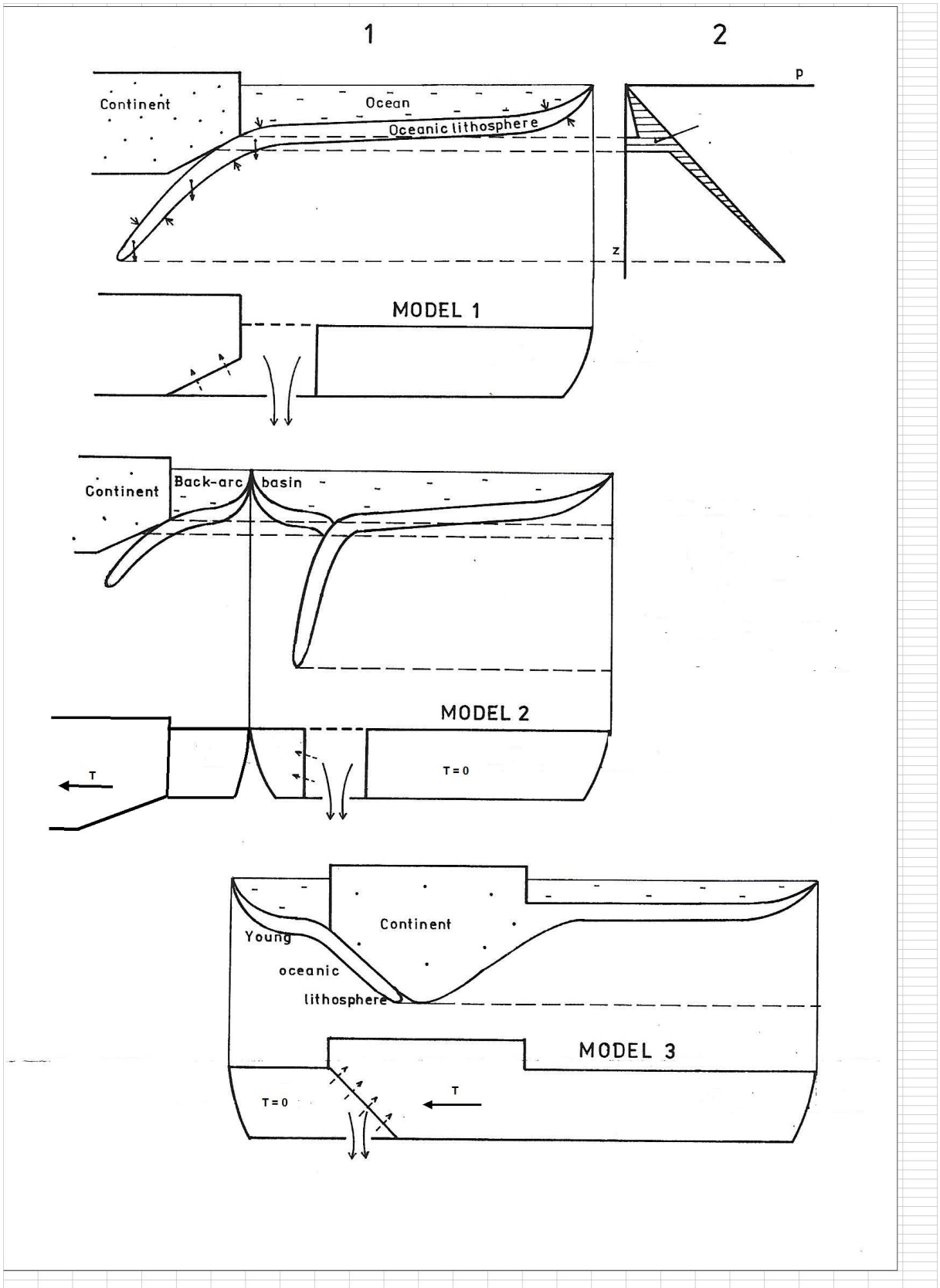

Figure 5. 1. Models of liquidation of oceanic lithosphere by subduction.

MODEL 1 represents the movement of the plate driven by tidal force to the free space released by the outlet of denser material through the hole. Dashed arrows mark light melted material uplifted to continent.

MODEl 2. Quick subduction of old oceanic lithosphere and receding of continent driven by tides T causes upwelling of asthenospheric material to the released space in the lithosphere and formation of back-arc basin with mid-ocean ridge.

MODEL 3. Overriding of young oceanic lithosphere by continent, provided that subduction started when the oceanic lithosphere was old.

Dashed arrows mark ascend of light melted component of oceanic lithosphere to the continent and full arrows mark the outflow of heavy material, solid and liquid through the hole. Action of tidal force T is explained in Fig. 2. for forces of equator-fleeing and tidal friction. Direction of resultant T is given by position of subduction zone, which releases free space for the plate movement.

2. Possible explanation of formation of forearc basins.

Small continents as Nazca and Cocos remain fixed on mantle. Philippine Sea is also small plate, but in its central part is relatively young, formed by light new material created by mid-ocean ridge in middle. Its origin is given by reality that the Pacific plate dropped down to mantle sooner before reaching continent. However, except central part, oceanic lithosphere is old and subducts. However, light central part forms obduction in Taiwan, because Philippine Sea plate is pushed by Pacific and Indo-Australian plates, explained in Fig. 6.

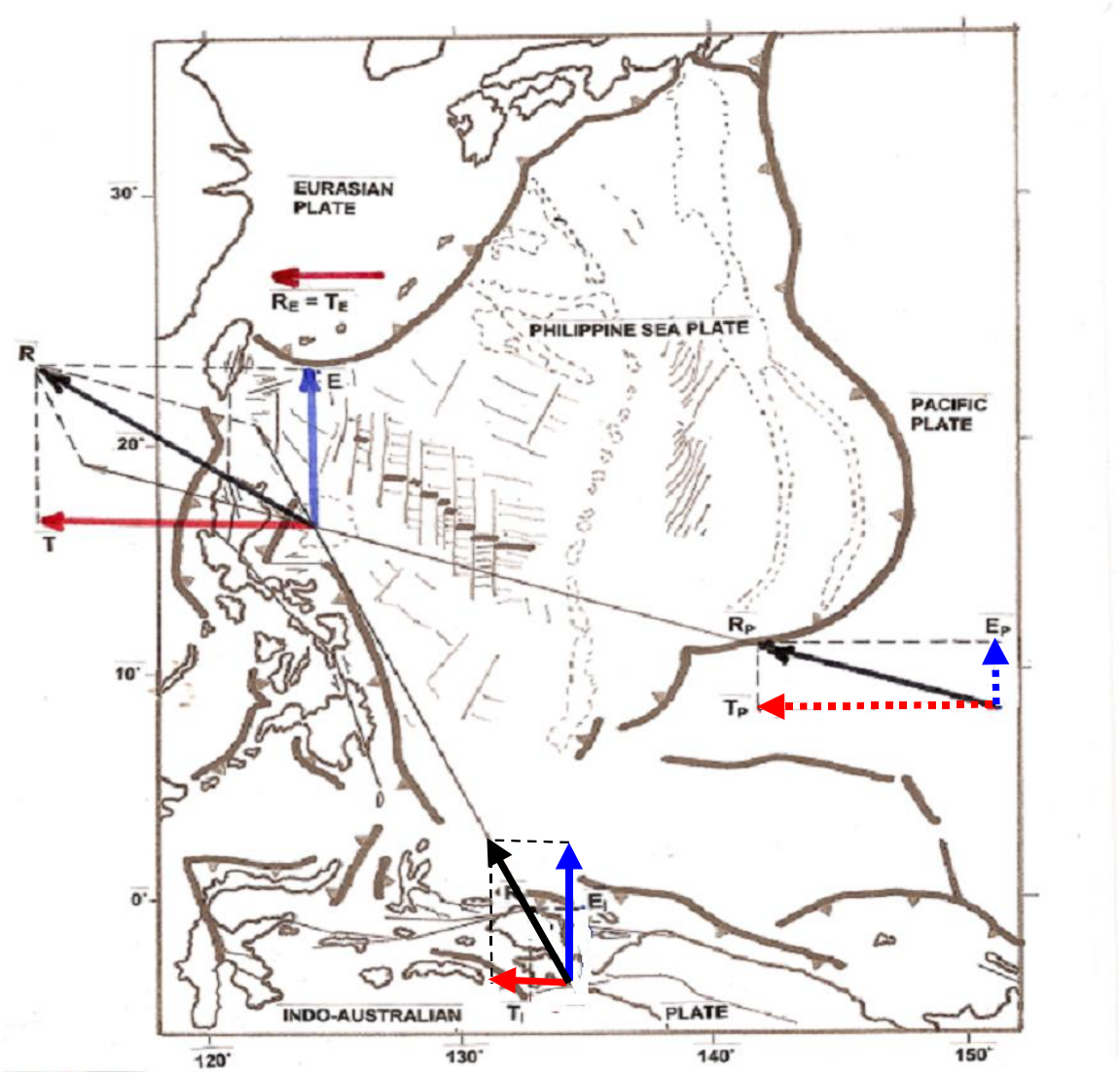

330

331

332 **Figure 6** shows the relative velocities of plates adjacent to the Philippine Sea plate taken from
333 the author's map (Fig. 3) of plate velocities in the reference frame considering the Nazca plate
334 as stable in point 50°S;100°W (Ostřihanský 1997, 2004). The resulting force folding rocks in
335 Taiwan is of NW direction; however earthquakes and direction of faults roughly
336 perpendicular show that the Philippine Sea plate is subjected to the tidal drag directing
337 westward and the equator-fleeing force directing northward. The Philippine Sea plate is
338 considered as only a buffer plate unable to move by means of own forces because it is too
339 small regardless that this plate is relative young (maximum 60 Ma), situated on 20°N, shifted

by the equator-fleeing force. Forces coming from the Pacific plate are plotted in dashed lines because the Pacific plate dropping down by gravity to mantle is not so effective as the Indo-Australian plate moving NNW. Alternating equator-fleeing force 10^{22} Nm (Fig. 2) moves effectively this small plate and pushes it together with westward component of Pacific plate to subduction zones on western side of the plate. Obduction is obvious because young and fossil mid-ocean ridge in the middle of Philippine Sea plate cannot subduct. (R, T, E are schematic expressions of resultants, of westward and equator-fleeing forces, with indexes for Pacific, Eurasian and Indo-Australian plates).

Heat flow on the Earth

The hypothesis that the heat-producing elements were strongly concentrated in the crust led to the prediction that the surface heat flow in the oceans, where the crust was known to be thin, would be considerably lower than the surface heat flow in the continents. Measurements by Revelle and Maxwell (1952) in the Pacific and by Bullard (1954) in the Atlantic showed that oceanic heat flow was very nearly equal to continental heat flow, so the prediction was not valid. Bullard et al. (1956) attributed this equality of heat flow to mantle convection. Global map of solid Earth surface heat flow (Davies 2013) clearly shows that increased heat flow in oceans is caused by uplift of hot mantle material in mid-ocean ridges, whereas in old oceanic lithosphere subducting areas the heat flow is extremely low. Extremely low hear flow can be found also in continents. Steady-state heat conduction is the only reasonable explanation of heat flow on the Earth. Uplift of hot material from mantle is facilitated by its change into liquid owing to Clapeyron Clausius equation in which decreased pressure leads to decrease of melting temperature. Therefore steady state heat

conduction and from it following thermal diffusion plays important role on the Earth. For example Schmucker (1969) presents for thermal conductivity 7 $Wm^{-1}K^{-1}$ and specific heat under constant pressure 1.1 J $K^{*1}g^{-1}$ that for time interval since Earth origin to present, the length of heat in conduction is only 860 km. Geology confirms that for example in Tertiary increased thermal flow could caused uplift of continents and subsidence of oceans, probably increased subduction and wide spread of dry land animals. Existence of low velocity zone (LVZ) support movement of plates even considering content of water (Takahashi and Kushiro, 1983). Considering asthenospheric material of viscosity 1.5×10^{20} Pa s (Schubert and Garfunkel, 1984), then really movement of plates is hardly possible. Nevertheless every Earth's rotation variations causes asthenosphere deformation and because every deformation is irreversible and deformation remains fixed by ascend of magma in mid-ocean ridge, creeping movement of plates is therefore inevitable.

Steady-state heat conduction in mantle is the only reasonable explanation of the heat flow on the Earth, It follows from my observatiions. In 1971-78 I preformed comprehensive study of relation between heat flow and heat production in Bohemian massif. (Ostřihanský, 1980) I found very low heat flow comming from depth 17.7 mW/m^2 whereas heat flow measured above batholiths ranged from 60 – 80 mw/m^2 owing to heat production from radioactive elements 2 – 8 $\mu W/m^3$. On the other hand in Bohemian massif exist volcannics of young age, for example Komorni Hurka (in German Kammerbühl) finished its activity only 10,000 years ago. For the first time I realized that the opening of volcano was the crossing of tectonic faults Krusne Hory and Sudets and therefore external force opened this volcano, i.e. tides. Result: Heat flow from mantle is low probably constant and volcanism and rapid heat flow increment is caused by tides, This concerns also oceans where created oceanic

lithosphere carries heat from opened faults. Kmorni Hurka is well known volcano where volcanic origin of basalt has been proven and opinions of neptunists rejected. (Meeting of J.W. Goethe with Sweedish chemist J J. Berzelius in 18th century).

Problem with origin of subduction

I must mentiion that mantle convection has its theoretical opponents. E.g. Jeffreys and Crampin (1970) formulated the Jeffreys-Lomnitz law, according to which large-scale damping does eliminate large active convection cells. To explain subduction of oceanic lithosphere rejecting mantle convection is not a simple task. Colder subcrustal rocks are sufficiently dense; the oceanic lithosphere founders and begins to sink into the interior of the Earth, creating the ocean trenches. To get through the mantle solid environment means that in fact it burns a hole in mantle (Fig. 5). Subducting oceanic lithosphere is a heat sink, on the other hand pressure-release producing melting and foundering of mantle facilitates the movement of downgoing slab. Imagination of bathyscaphe can substitute the solid and heavy sinking oceanic lithosphere. It prevents increase of intrinsic pressure, but the heat streams inside, where temperature several thousands ºC creates not only basaltic melt but basaltic gas, i.e. explosion, which directs downward because upper part of ocanic lithosphere is solid anf firm. Liquidation of oceanic lithosphere in subduction zones is one of basic prepositions of lithospheiic plates movement by tides. Only plates released by subduction can move by tides. There is no mantle convection, only buoyancy uplift of

414 produced magmas for volcanic arcs streams simply upward and there is no mantle
415 flow driving down subducted slab.
416
417 **Action of tides on the Earth**
418
419 At present time there are known two phenomena on the Earth, which are evidently
420 influenced by tides, there are Earth rotation variations and direct measurements of
421 distances on Earth by means of Global Navigation Satellite System (GNSS). Yoder et
422 al., (1981) identify periodic variations of the Earth's rotation due to tides (zonal) with
423 maximum amplitudes (Table 1).
424
425
426 **Table 1**

Period days	Explanation	Amplitude $\times 10^{-7}$ s
-6790.36	Moon nodal period 18.61 years	1720,498
-3399.18	Half Moon nodal period	-8,404
3232.85	8.85 years	-43
1305.47	3.57 years	-449
365.26	One year	16,339
182.62	6 months	51,327
121.75	4 months	2,005
27.56	Sidereal Moon's period	8,785
13.66	½ Moon's sidereal period	8,252
9.13	⅓ Moon's sidereal period	1,056

But (Zaccagnino et al., 2020) uses from Cartwright and Edden (1973) and Kudryatsev (2004) following amplitudes for baselines (Table 2).

Table 2

Period days	Explanation	Amplitude (m)
6798.659	Moon nodal period 18.61 years	0.07119
3399.329	Half Moon nodal period	0.00064
3232.605	8.85 years	0.0003
1305.756	3.57 years	0.0009
365.264	One year	0.01360
182.625	6 months	0.08565
121.752	4 months	0.00426

Table 1 shows tides responsible for the speed of Earth's rotation. Table 2 shows tides acting in driving lithospheric plates. Analysis of Zaccagnino et al.,(2020) shows that the largest period, the nodal 18.61 years with largest amplitude is not evident, but evident are: the half Moon nodal period 1305 days, one year period, half year period and ⅓ year period. The Yoder's et al. table from which data from Table 1 are taken has headline: Periodic Series for –ΔUT1, it means that positive values of amplitudes are decelerating variations and negative accelerating variations. Periods are positive with exception of nodal periods, which are negative owing to negative nodal movement. Therefore half nodal amplitudes are in fact positive but nodal period with

highest amplitude is negative and for this reason in Zaccagnino et al., graphs the full nodal amplitude is not evident directing to negative values.

Practicly, the Moon nodal tidal period 18.61 years is evident in westward driving plates. Fig. 7 shows repetition of earthquakes Norcia 1979 (a), Norcia 1989 (b), Colfiorito 1997 (c), L'Aquila 2009 (d) and Rieti 2016 (f) with possible earthquake prediction 2034. Earthquakes Norcia 1989 (b) and L'Aquila 2006 (d) are triggered by resonance effect. Fig. 7 does not show earthquakes magnitude but number of earthquakes. Tides are not responsible for earthquakes magnitude, this is affected by material properties prone to trigger earthquake. Number of earthquakes better characterizes tidal influence.

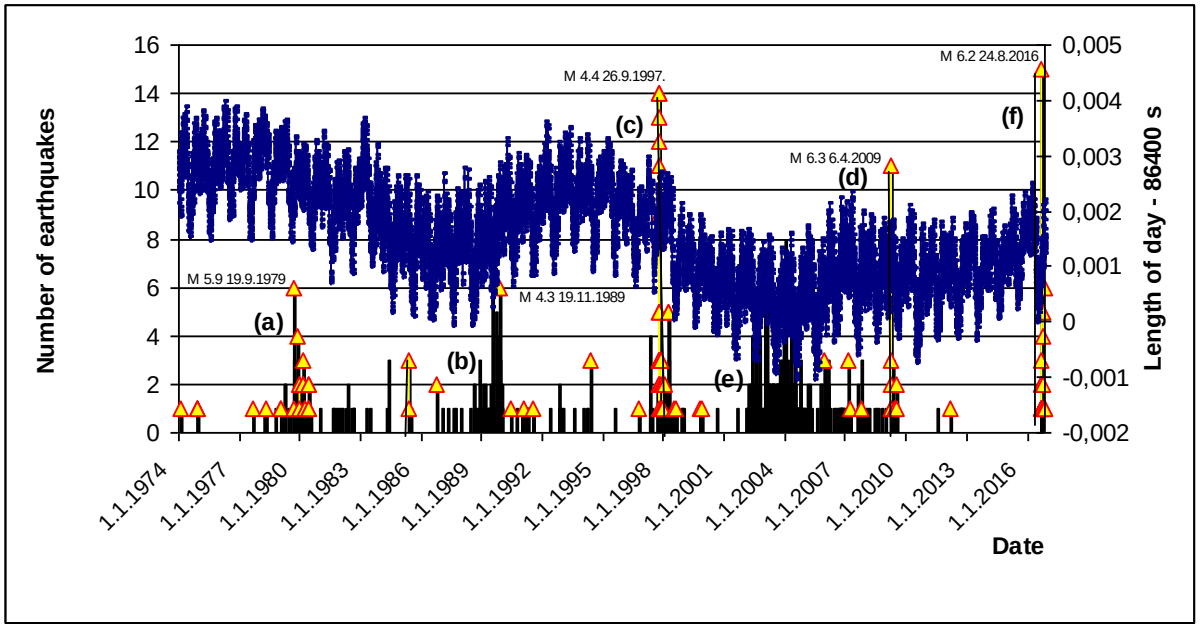

Fig. 7. The length of a day record and the occurrence of earthquakes in the Norcia-Marche-Abruzzi region for the period 1974-2016. The areas of increased earthquakes activity correspond to the Norcia 1979 (a), Norcia 1989 (b), Colfiorito 1997 (c), L'Aquila 2009 (d)

and Rieti 2016 (f) earthquakes and to the continuous earthquake occurrence inperiod 2002-2005 (e). Earthquakes of magnitude M>4 are marked by triangle

Figure 7 represents histogram, therefore maxima of 18.61 years period are statistically significant. and expectaton of next earthquakes enlargement in 2034 is probable.

Strong dependence on ½ Moon's sidereal period (13.66 days) shows Fig. 8 for enormously quick Earth rotation, period 2002-2005, position (e) on Fig. 7. i.e. for positive and negative Moon's declinations.

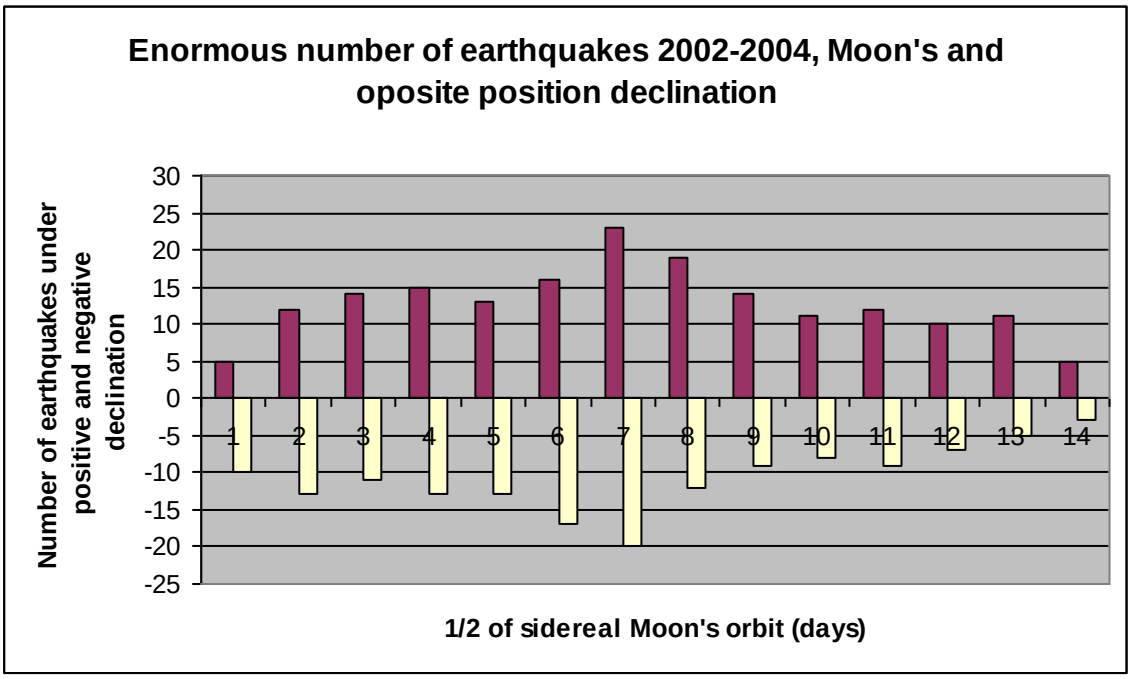

Fig. 8. Histogram of earthquakes occurrence in dependence of Moon's position of its orbit. Remark: Numbers on y-axis are real number of earthquakes not values of declination in degrees. Earthquakes are taken from ANSS Catalog over 3 rd magnitude from period of very high Earth rotation speed 2002 – 2004 (minimum of LOD marked by (e) on Fig. 7). Moon's position on its orbit has been simply found plotting earthquakes on LOD graph and counting number of days between two LOD maximums for every earthquake, for both positive and negative declination part of LOD graph. This is the simplest and quickest proof of earthquakes triggering by tides.

Earthquakes in Fig. 8 are taken from ANSS Catalog over 3 rd magnitude from period of very high Earth rotation 2002 – 2004 (minimum of LOD marked by (e) on Fig. 7). Moon's position on its orbit has been simply found plotting earthquakes on LOD graph and counting number of days between two LOD maximums for every earthquake, foror both positive and negative declination part of LOD graph. This is the simplest and quickest proof of earthquakes triggering by tides. Compare very close similarity of LOD and Moon's declination graphs on Fig. 17.

Similar predictions can be done for Alaska's earthquakes (Fig. 9), where it is difficult to distinguish 18.61 years Moon nodal cycle from Metonic cycle 19 years. Prediction for next earthquake in South Central Alaska is for 2021.

It would be an error to suppose that earthquakes on the whole Earth should be triggered in e.g. lunar major stand still when Moon's declination reaches maximum, in May 1988, June 2006, April 2025 and September 2043. Repetition of earthquakes in 18.61 years period is evident, nevertheless beginning of the period depends on constituents causing direction of the plate movement. Similarly solid Earth tides or ocean tides cause diurnal maximum uplift not in Moon's transfer over meridian, but in shift for several hours considering all tidal constituents. Therefore Central Italy has earthquakes 1979, 1997, 2016 and 2034, disturbed by resonance Norcia1989, L' Aquila 2006 and unknown earthuake 2028. South Central Alaska has earthquakes 1964, 1988, 2002 and 2021.Repetition of earthquakes is not evident in Indo-Australian plate. Only one repetition has occurred for Great Sumatra earthquake 26. December I.2004 and Sumatra earthquake 27 December 1985 M 6.6. The exact time span 19 years indicates the Metonic cycle and details show the exact positions

of full Moon, winter solstice, maximum Moon's and Sun's declination and maximum Earth's rotation speed and similar character of aftershocks. Such position however does not occur every 19 years because maximum torque depends on full Moon and also on maximum Moon's declination varying in 18.61 years nodal cycle. Coincidence both parameters $s = t_1 \times t_2 / (t_2 - t_1) = 18.61 \times 19/(19-18.61) = 900.6$ yr. Except resonance, beats play role in earthquake triggering (More information, Ostřihanský, 2015).

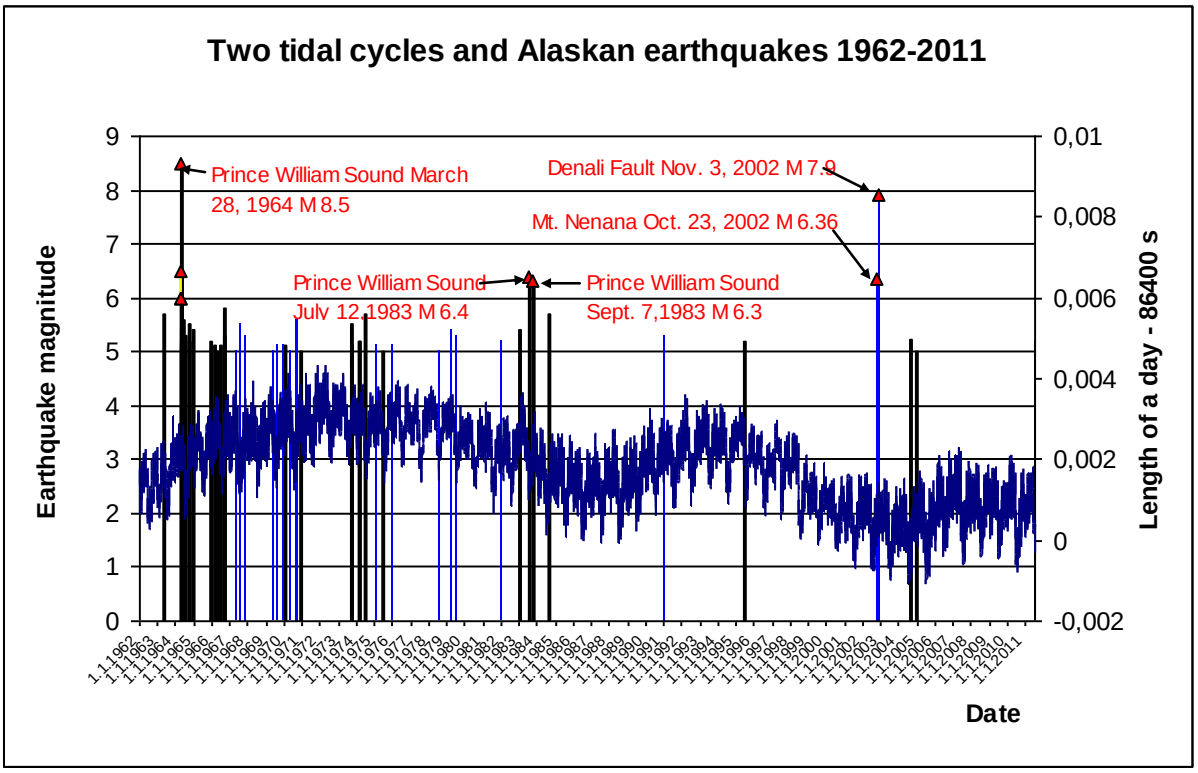

Fig. 9. The figure shows two 19 years Metonic cycles in Alaska 1964-1983 and 1983-2002. Cycles are bordered by earthquakes M 8.5 Prince William Sound March 28, 1964, M 6.4 Prince William Sound Jul. 12, 1983 and M 7.9 Denali Fault Nov. 3, 2002. Blue bars mark earthquakes from area of the Denali fault. The first Metonic cycle is characteristic by area of increased LOD and large number of earthquakes resembling aftershocks of M 8.5 earthquake

but they can be explained as originated in any Earth's velocity increment from the slow movement. The investigated area covers rectangle 60° N – 65° N, 146° W - 149°W with Anchorage and Fairbanks. Triangles mark earthquakes >M6.

Complications with earthquake prediction and in estimation of tidal origin of earthquakes:

Tides to drive plates, plates should be released and this release is manifested by dropping down of oceanic lithosphere by gravity to mantle. Because at present time subduction zones of oceanic lithosphere were created on the northern part of lithospheric plates, plates move northward. But tidal friction drives plates westward, supposing of course that they have subduction zone on their western side.

Complicated situations are created not only in Sun and Moon action in different mutual hour angles, but also in their action during diurnal cycle in New or Full Moons (Table 3).

Table 3

	Phase	Moon Declination	**0 h**	**12.4 h**
Summer	**Full**	**+**	$+M -S_c$	$-M_c+S$
S>0	Moon	**-**	$-M -S_c$	$+M_c+S$
	New Moon	**+**	$+M +S$	$-M_c-S_c$
		-	$-M +S$	$+M_c-S_c$
Winter	**Full Moon**	**+**	$+M+S_c$	$-M_c -S$
		-	$-M +S_c$	$+M_c-S$
S<0	**New Moon**	**+**	$+M -S$	$-M_c+S_c$
		-	$-M -S$	$+M_c+S_c$
Spring **S=0**		**+**	$+M$	$-M$
		-	$-M$	$+M$
Fall **S=0**		**+**	$+M$	$-M$
		-	$-M$	$+M$

Table 3 shows possibilities of earthquakes triggering during Full or New Moon and in summer and winter time. Example: In winter and in Full Moon the torques of Moon and Sun are added as shown in rectangle with bold contours. Similar situation is in New Moon, Moon and Sun torques are negative but earthquake triggering occurs for 12.4 hours later. M and S are Moon and Sun torques proportional to Moon and Sun declinations, M_c or S_c are Moon and Sun counterparts. Following figures present explanation. .

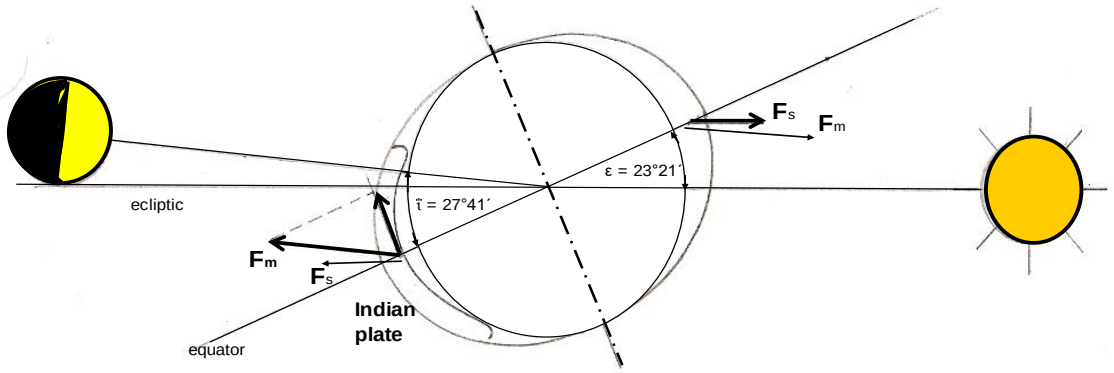

574

575

576

577

578 **Figure 10** shows Full Moon, maximum Moon's declination 27º 21´ and the torque acting on
579 Indian plate directs northward. 12.4 hours later torques direct southward (not marked in
580 figure) against mid-ocean ridge and no earthquakes are triggered. This is the case of Great
581 Sumatra earthquake 2004. Moon's torque (F_m =M) directs northward and also the Sun's
582 counterpart S_c=$F_{s)}$, as evident in wintertime.

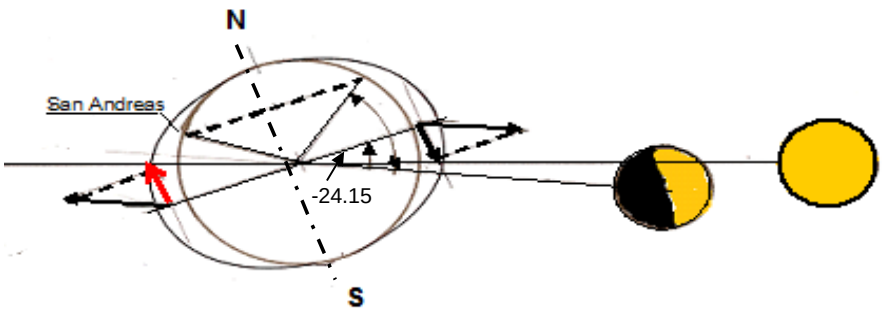

583 **Figure 11.** Case of New Moon in winter, when Sun's and Moon's declinations are negative
584 (Moon –24.15º), but earthquakes are triggered for 24.4 hours later (marked by red arrow).
585 Black arrow direct southward against mid-ocean ridge without any earthquake or the plate
586 movement.
587
588 There are questions whether Full or New Moon trigger earthquakes. Statistics of
589 Van der Elst at all. (2016) confirm it, but Hough, (2018) not. Looking at Table 3, it is
590 evident that not all Full or New Moons have sufficiently strong torques to trigger
591 earthquakes. Probability is about 50 % because in summer and in winter there are
592 only two possibilities of summarizing Moon and Sun torques (in bold contours), in
593 remaining possibilities, Moon and Sun torques are subtracted. One more property
594 follows from the Table 3: In summer for New Moon, Sun's torque S is summarized
595 with Moon torque M. In winter for Full Moon, Moon torque M and Sun's counterparts
596 S_c are summarized and trigger earthquake, For summer part it is interesting that for
597 Full Moon, the Sun's torque is subtracted (i.e. directs south) and for the time when
598 also Moon's torque directs southward (has negative torque), then waiting 12.4 hour,
599 both counterpart summarized torques direct northward, triggering strong earthquake.
600 Figures 10 and 11 depict Full and New Moon positions for wintertime. Reader easily
601 imagines configurations for summer with Sun's position above equator.
602 Tidal friction acts on plates semi-diurnally and westerly with very weak torque 10^{16}
603 Nm as calculated. This can be considered as permanent action (similar as pressure
604 of hand on drilling hammer) but drilling itself is performed by far stronger variations

(electric or pneumatic device), in our case north-south tidal variations 10^{22} Nm (see scheme on Fig. 2). Load situated on inclined level surface, kept by friction but introduced into movement by strong variations, is a very good example of it. However lithospheric plate can move only if its front part is released by dropping down by gravity in subduction zone. Hawaii-Emperor Seamount chain has changed its direction owing to the change of position of subduction zone. All these examples are documented in author's paper (Ostřihanský 2015).

Consequent earthquake tidal triggering

To elucidate tidal action on earthquake triggering, let us consider three dominant faults on the Earth: Matawai Fault on Sumatra, Palu-Koro Fult on Sulawesi and San Andreas Fault in California (Fig. 12). Tidal periodicity is evident; first started the earthquake San Andreas Fault 8.IX.2004**, one Moon sidereal period** (27.56 days later) earthquake 5.X.2004, further **4 sidereal periods** Sumatra 26.XII.2004 and ended **one sidereal period** Sulawesi 23.I.2005.

Great Sumatra earthquake is situated exactly in LOD minimum (Fig. 12a), corresponding to extreme positive Moon's declination 27.9º and negative Sun's declination close to winter solstice -23º, forming the Full Moon configuration of maximum tidal torque. New Moon coincides with next LOD minimum 13.66 days later with Moon's negative –27.9º declination and almost unchanged Sun's negative declination with maximum tidal torque at 12.4 hours later (the last bold contours rectangle of winter, Table 3). The next LOD minimum is 23.I.2005 with 26.0º Moon's declination and the Full Moon in close position 25.I.2005. However the maximum earthquake does not correspond to LOD minimum, but is shifted for three days on

position 27. and 28. I. 2005. The explanation is difficult; it is evident that only the third diurnal stroke triggered the earthquake. The shift from LOD minimum to LOD maximum is evident on earthqauke Sumatra 28.3.2005 (Fig. 13) as consequent action of westward plate movement by tidal friction.

Transferring our attention to the Palu-Koro Fault, it is evident (Fig.12b) the earthquake 23.I.2005 corresponds to LOD minimum exactly, situated in 2000 km distance from Mentawai Fault in Sumatra. Whereas expressive LOD minimums on Sumatra and Sulawesi are empty of earthquakes (Figs 12ab left), the LOD minimum 8.IX.2004 on San Andreas Fault (Fig. 12c) has earthquakes with aftershocks. Moon has maximum positive declination 27.8º. Low Sun's declination 5.4º in close position to autumn equinox and Moon in last quarter minimizes any influence of Sun.

Maximum westward tidal drags occur in Moon and Sun position on equator at 0º declination, i.e. in LOD maximums. Earthquakes increment occurred in San Andreas Fault 29.IX.2004 coinciding exactly with LOD maximum 29.IX.2004 (Fig.12c) with Moon's declination 6.4º and Sun's declination –2.6º. Next earthquake increment occurred in LOD minimum 5.X.2004 with declination 28.0º, corresponding to tidal north-south variation and further earthquake increment occurred till the end of December. The westward movement of the American plate is confirmed by earthquake one day before 28.IX.2004 (green color Fig. 121c) at depth only 7.9 km, whereas earthquakes of San Andreas Fault occur in average depth 30 km. The next LOD maximum occurred 3.I.2005, but earthquake increment occurred for 2 days later 5.I.2005 (Fig. 12c).

a

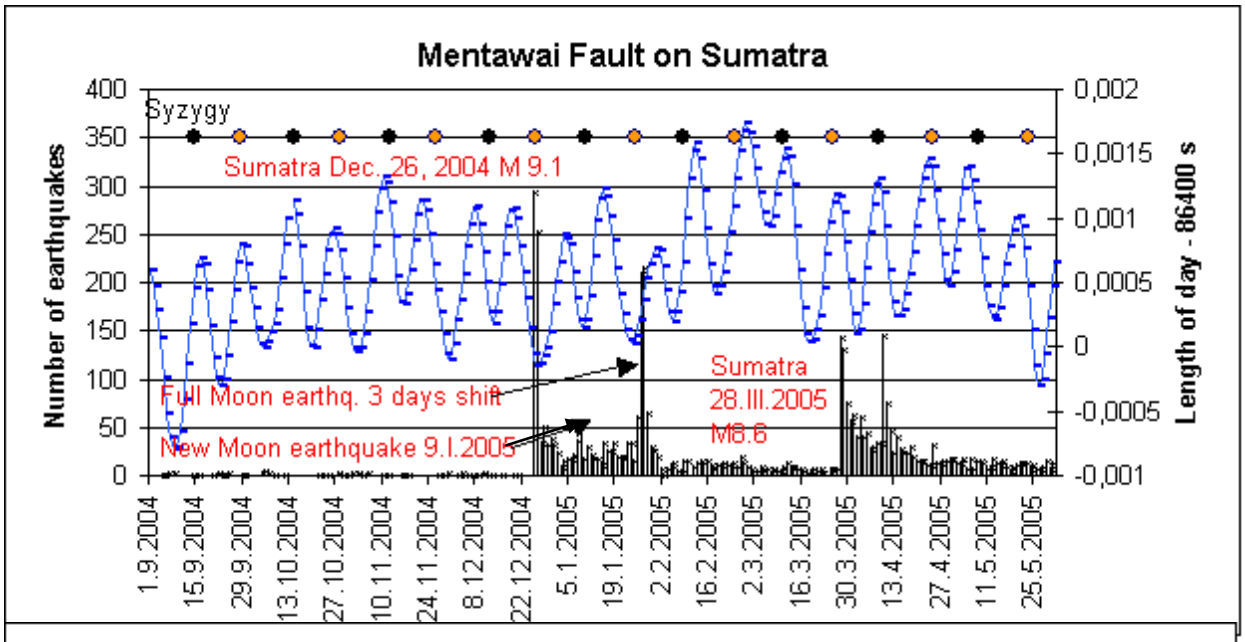
Mentawai Fault on Sumatra
Syzygy
Sumatra Dec. 26, 2004 M 9.1
Full Moon earthq. 3 days shift
New Moon earthquake 9.I.2005
Sumatra
28.III.2005
M8.6
Number of earthquakes
Length of day - 86400 s
400
350
300
250
200
150
100
50
0
0,002
0,0015
0,001
0,0005
0
-0,0005
-0,001
1.9.2004
15.9.2004
29.9.2004
13.10.2004
27.10.2004
10.11.2004
24.11.2004
8.12.2004
22.12.2004
5.1.2005
19.1.2005
2.2.2005
16.2.2005
2.3.2005
16.3.2005
30.3.2005
13.4.2005
27.4.2005
11.5.2005
25.5.2005

b

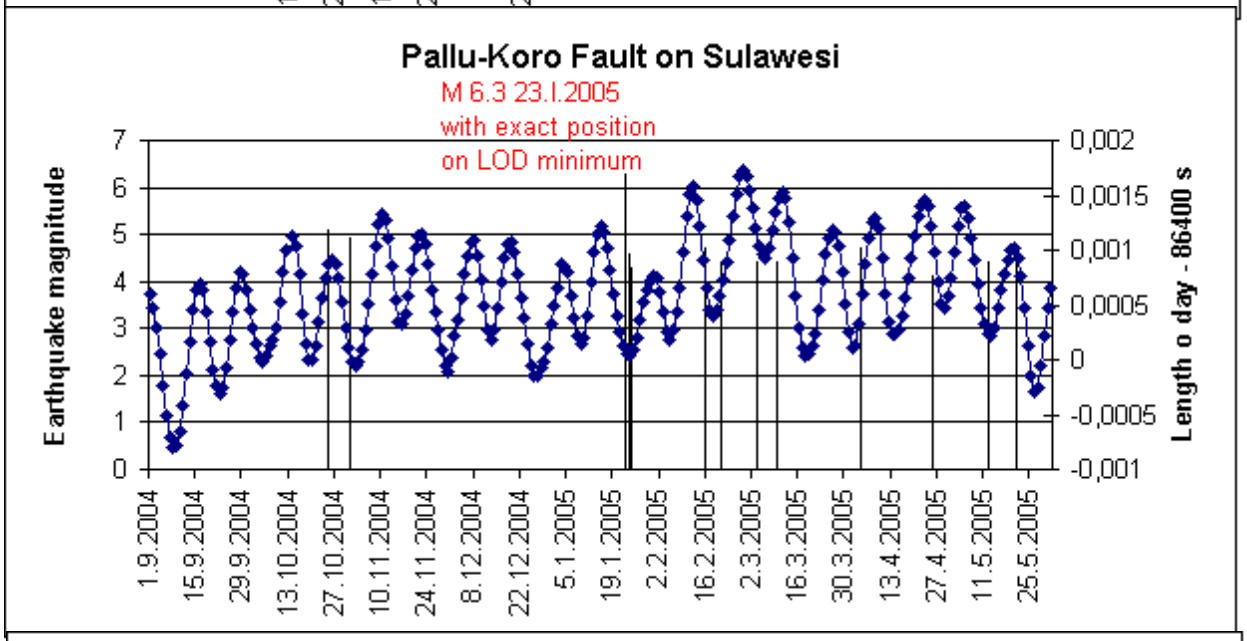
Pallu-Koro Fault on Sulawesi
M 6.3 23.I.2005
with exact position
on LOD minimum
Earthquake magnitude
Length o day - 86400 s
7
6
5
4
3
2
1
0
0,002
0,0015
0,001
0,0005
0
-0,0005
-0,001
1.9.2004
15.9.2004
29.9.2004
13.10.2004
27.10.2004
10.11.2004
24.11.2004
8.12.2004
22.12.2004
5.1.2005
19.1.2005
2.2.2005
16.2.2005
2.3.2005
16.3.2005
30.3.2005
13.4.2005
27.4.2005
11.5.2005
25.5.2005

c

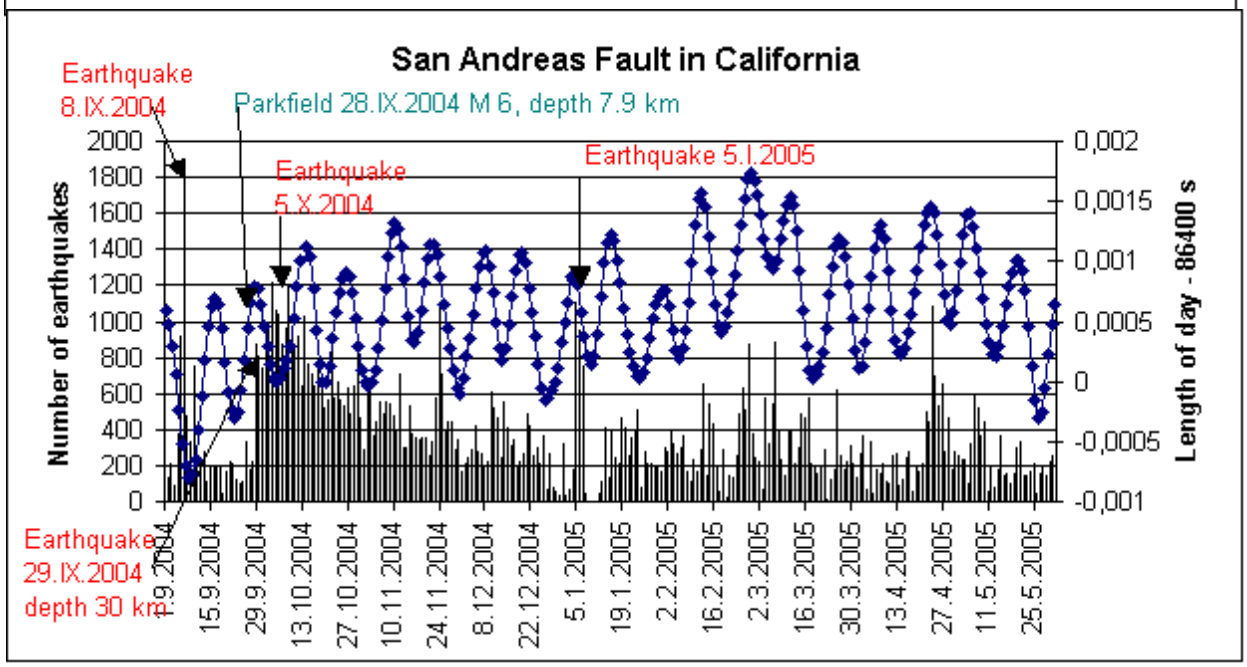
San Andreas Fault in California
Earthquake
8.IX.2004
Parkfield 28.IX.2004 M 6, depth 7.9 km
Earthquake
5.X.2004
Earthquake 5.I.2005
Earthquake
29.IX.2004
depth 30 km
Number of earthquakes
Length of day - 86400 s
2000
1800
1600
1400
1200
1000
800
600
400
200
0
0,002
0,0015
0,001
0,0005
0
-0,0005
-0,001
1.9.2004
15.9.2004
29.9.2004
13.10.2004
27.10.2004
10.11.2004
24.11.2004
8.12.2004
22.12.2004
5.1.2005
19.1.2005
2.2.2005
16.2.2005
2.3.2005
16.3.2005
30.3.2005
13.4.2005
27.4.2005
11.5.2005
25.5.2005

Figure 12. LOD graph and earthquakes during half-year from 1.IX.2004 to 31.V.2005. LOD maximums show dominantly Moon's 0º declinations, LOD minimums alternatingly positive and negative Moon's declinations. As evident, the reason for triggering of these three earthquakes was the Moon's high declination during the 18.61 years Moon's nutation cycle. Plotted earthquakes of San Andreas Fault are low frequency earthquakes of 15 years Catalog of Shelly (2015) in average depth 30 km. Earthquake 28.IX.2004 in 7.9 km (in green) is from ANSS Catalog. This corresponds to westward driving American plate. Sumatran earthquakes from ANSS Catalog are plotted as umber of earthquakes/day for comparison. Earthquakes from Palu-Koro Fault taken from ANSS Catalog, had minimum aftershocks and measure in earthquakes magnitude has been found more suitable. Tidal periodicity started with San Andreas Fault 8.IX.2004**, one Moon sidereal period** (27.56 days later) earthquake 5.X.2004, **4 sidereal periods** Sumatra 26.XII.2004 and **one sidereal period** Sulawesi 23.I.2005.

These earthquake-triggering delays are very common in LOD maximums and detailed investigation of earthquake Sumatra M 8.6 28.III.2005 shows the tidal origin of these earthquakes (Fig. 12a right and detail Fig. 13). In this example the mechanism of tidal earthquakes triggering is well evident. North-south movement along Mentawai Fault and the great drop along subduction zone with tsunami manifest the Great Sumatra earthquake M 9.1, 26.XII.2004. For three months later the released Indian plate moved westward overriding subduction zone and triggering earthquake Sumatra M 8.6 28.III.2005, but without tsunami.

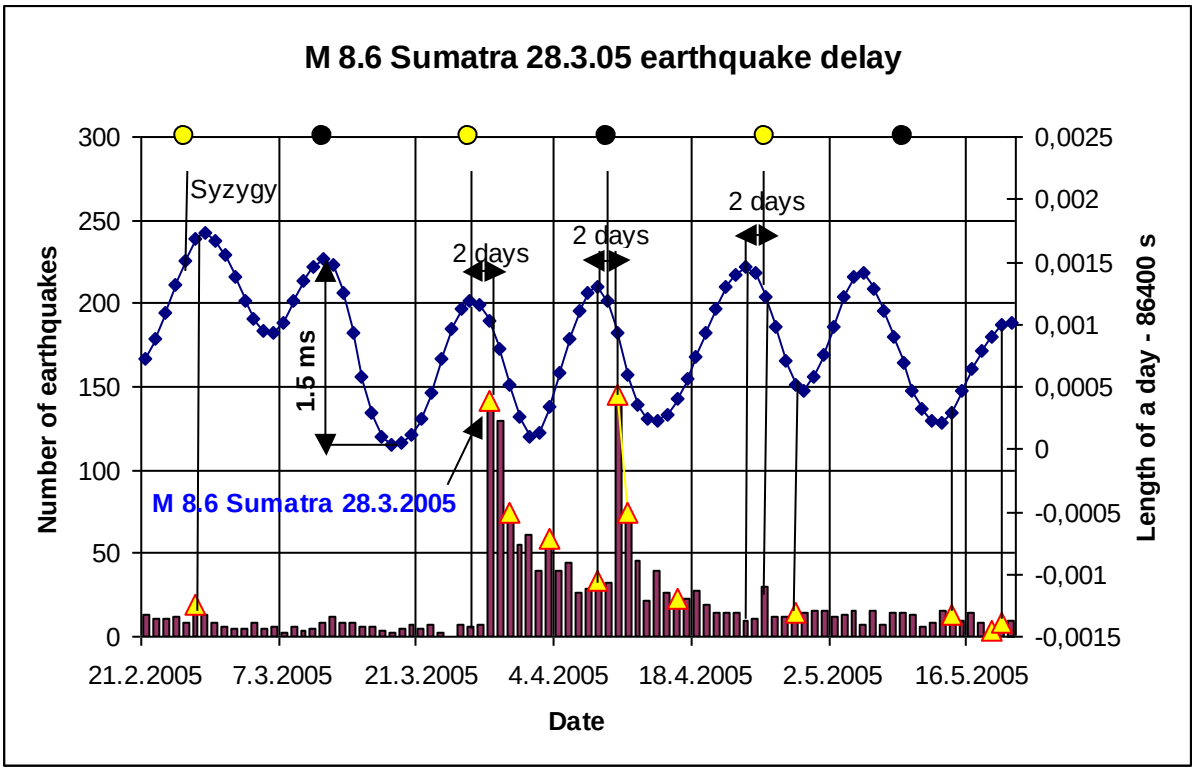

Figure 13. Coincidence of LOD maximum with Full Moon is evident as maximum dragging factor of Moon and Sun situated on equator for westward tidal drag. However 2 days delay is evident for all three earthquakes increments repeating in sidereal half 13.66 days periods. Westward movement created this earthquake, but repetitions of aftershocks in sidereal Moon's cycle confirms influence of north-south movement supporting westward tidal friction. Plotted earthquakes are from AMSS Catalog.

There are some questions, which remain to explain: The Sumatran earthquake of New Moon 10.I.2005 was triggered exactly in LOD minimum and minimum declination –27.9º in agreement with Table 3. The same conditions fulfills

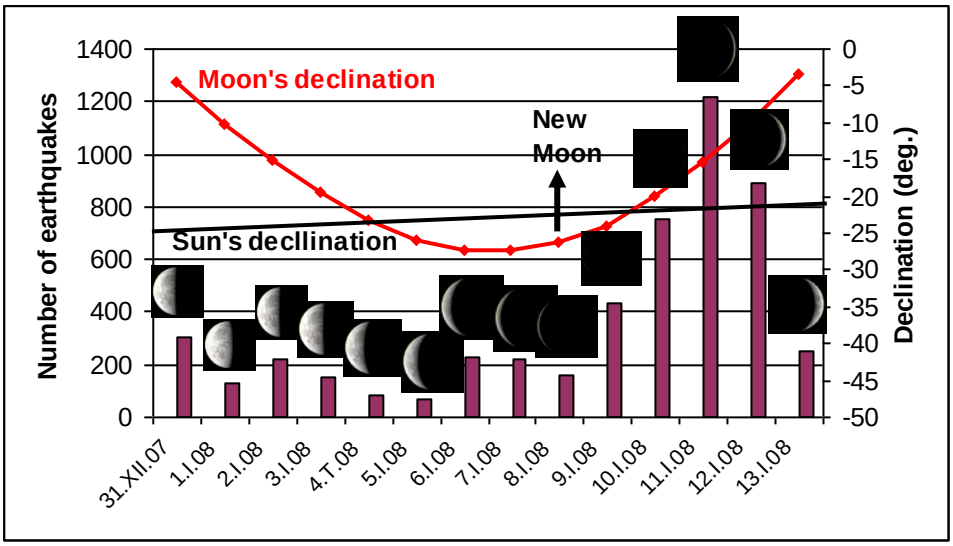

687

688

689 **Figure 14** shows earthquake delay for 3 days after New Moon and 4 days after Moon's
690 declination minimum (-27.5º) 7.I.2008 in configuration of winter time in Table and
691 earthquake triggering 11.I.2008. Plotted earthquake from 15 years Shelly (2017) Catalog are
692 exposed as histogram/day. LOD graph (see Supplement) shows negligible difference from
693 plotted Moon's declinations, considering almost constant Sun's declination.

694

695 the New Moon earthquake in San Andreas Fault 11.I.2008 but with 4 days delay, as
696 Fig. 14 depicts. Before earthquake 11.I.2008 long quiet period existed and the
697 earthquake was triggered only after the fourth diurnal stroke. Nevertheless solution
698 can be far complicated. Let us see Figure 15, which shows 57 syzygies and about 6
699 earthquake increments up to 800 earthquakes/day. Only New Moon 11.I.2008
700 correlates with earthquakes increment with negative Moon and Sun declination
701 according last row in Table 3 for winter S<0. If earthquake occurs on LOD maximum
702 (at 0º declination) then earthquakes in Full Moon or New Moon are not triggered,
703 because all tidal energy has been consummated for westward movement by tidal
704 friction (Fig. 17). (See also Fig. 15a in Ostřihanský, 2019). Fig. 15 shows that

earthquake triggering in Full or New Moon is phenomenon relatively scarce. Details show (see Supplement) more frequent earthquakes with maximum declinations and torques without contribution of Sun's torque, but also two earthquakes 18.XII.2008 and 16.VI.2009, which were triggered exactly at 0º declination and following New Moons are absolutely without any earthquakes.

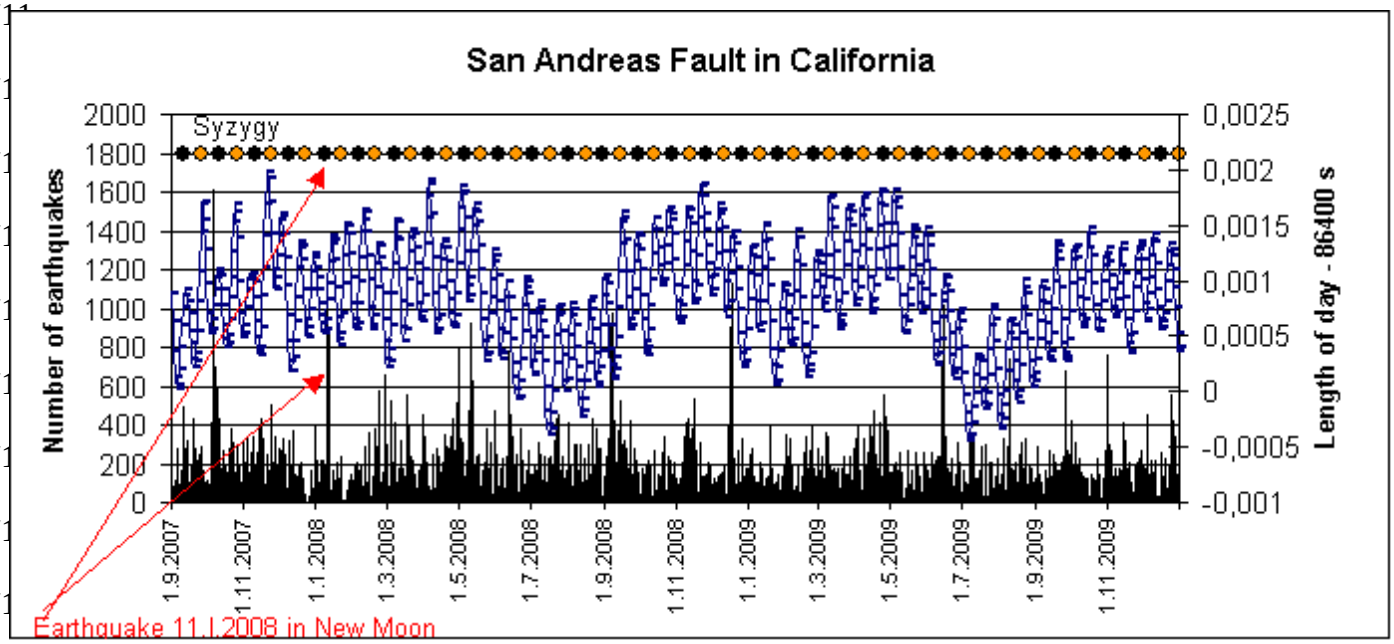

Figure 15 shows that coincidence of syzygies (Full or New Moon) with earthquakes are more likely extraordinary, as shows this shorter time span from IX. 2007 to XII. 2009. Only New Moon 11.I.2008 correlates with earthquake but with 3 days delay. More likely earthquakes correlate with LOD extremes, i.e. Moon's extreme declinations. However Van der Elst et al. (2016) proved correlation with szyzgies for time span 2008 – 2015. Earthquakes positions are taken from 15 years Catalogue of Shelly (2017). Supplement shows details on San Andreas Fault 1.IX.2007 – 31.XII.2009.xls.

729 Fig. 16 shows earthquake triggering during New Moon and Full Moon, where
730 cooperation of Sun's torque is evident. In Moon's last quarter the Sun's torque is
731 minimized also owing to minimum Sun's declination in vernal equinox, but Moon's
732 torque itself is able to trigger earthquake.
733

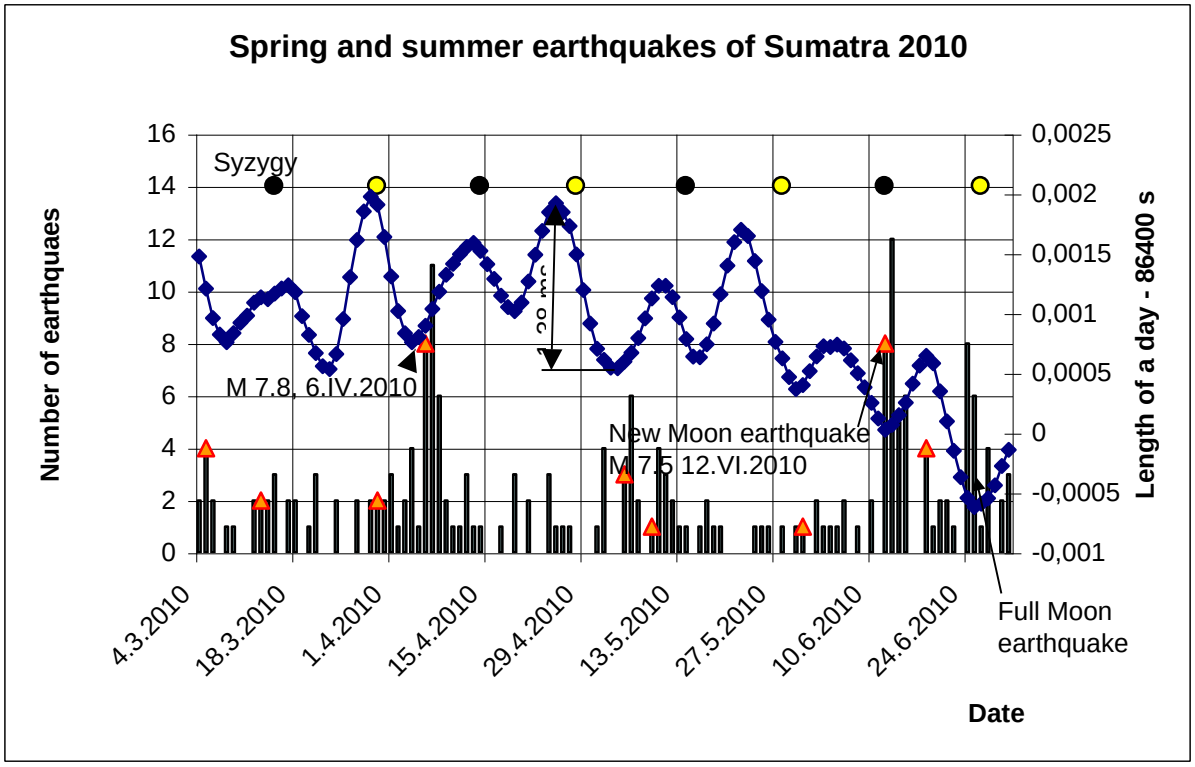

734
735

736 **Figure 16.** In contrast to New Moon earthquakes of Sumatra and San Andreas Fault triggered
737 in winter time with negative declinations –27.9º and –27.5º (Figs. 12 and 13), the New Moon
738 earthquake M 7.5 12.VI. 2010 has Moon's positive declination 25.0º and Sun's 23.0º, fully in
739 agreement with Table 3 for earthquakes in summer time because this earthquake was
740 triggered 7 days before summer solstice. Spring earthquake M 7.6, 6.IV.2010 in Moon last
741 quarter has declination –25.2º and was triggered 12.4 hours later according to Table 3 (+M).
742 Full Moon earthquake, without stated magnitude, has Sun's positive declination and Moon's
743 negative declination. Earthquake was triggered 12.4 h later with Sun's torque and Moons

744 counterpart M_c moving plate northward in agreement with Table 3. Triangles mark
745 earthquake over M 5.5. Earthquakes are taken from ANSS Catalog.

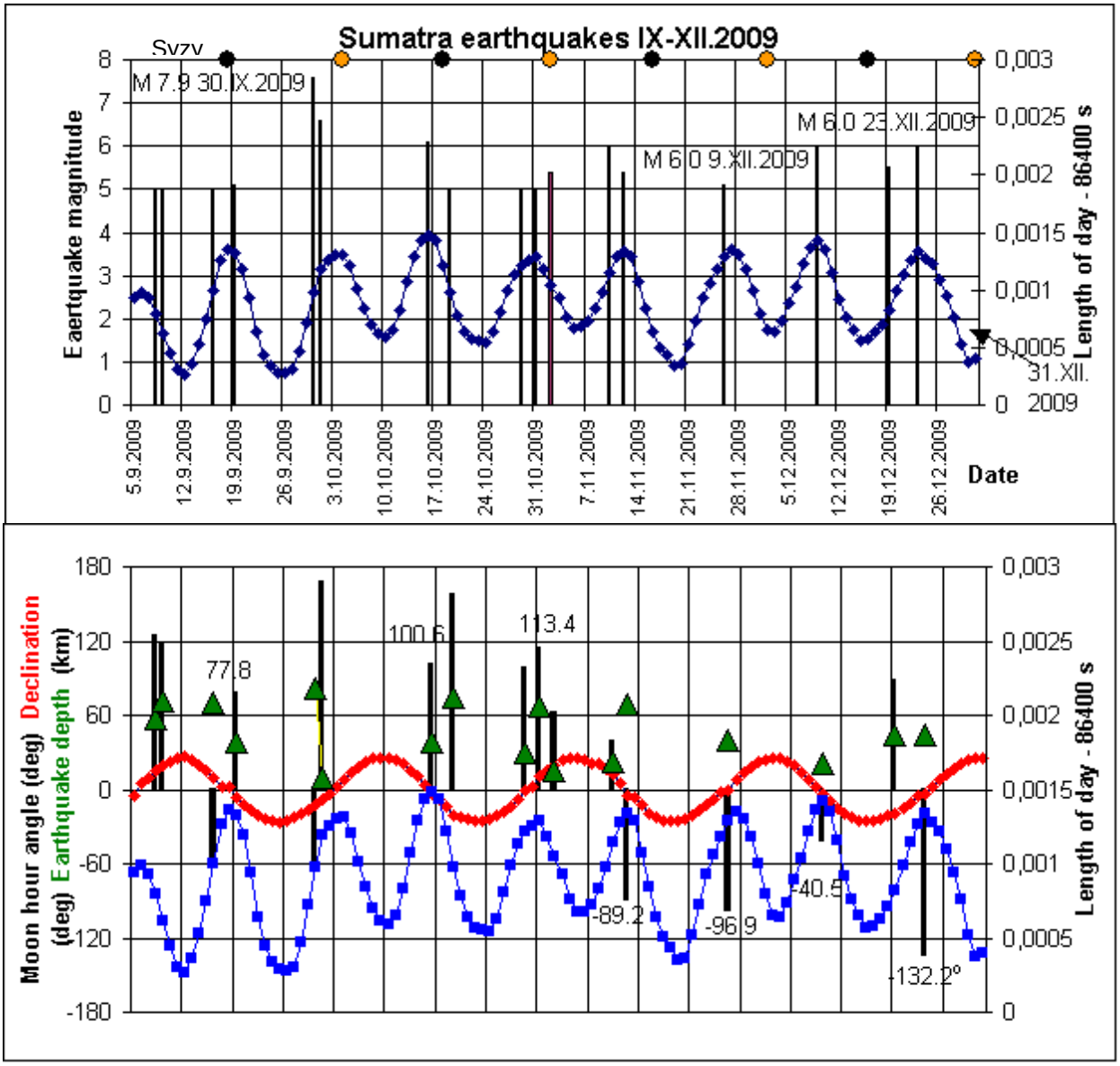

746

747 **Figure 17**. Excellent conditions for earthquakes triggering of Full Moon 31.XII.2009 and one
748 sidereal month before, **exhibit no earthquakes** in LOD minimums with positive Moon's
749 declination and negative Sun's declination in wintertime, the same conditions which were in
750 Great Sumatra earthquake 26.XII.2004. The reason is following; the triggered earthquake at
751 0º declination documents that all tidal energy was consummated for the westward plate
752 movement by tidal friction. Figure exhibits consequent transfer from north-south movement

to westward drag. Earthquakes positions and depths are taken from ANSS Catalog, Moon's declinations and hour angles are taken from Sun and Moon position Calculator on Internet,

The last Figure 17 shows westward directing tidal drag, acting for several months, represented earthquakes at 0º declination and no earthquakes under Full or New Moons. LOD minimum 31.XII.2009 represents exact position of Full Moon with large positive declination of Moon 25.8º and negative declination of Sun –23.1º but no earthquake. Tidal friction triggers earthquakes at 0º declination (LOD maximum) M 6.0 23.XII.2006, M 6.0 9.XII.2009 and some others during fall 2009 at 0º declination or close to this position.

Conclusion and discussion

Tides trigger earthquakes and move lithospheric plates. The Earth is not homogeneous body with estimated Rayleighs numbers and other materials characteristics but covered by plates movable by subduction, releasing free space for movement. Failure in estimation of tidal origin using theoretical Earth properties lead to consideration the Earth as the thermal engine with mantle convection as the plate driver. Mantle convection in Earth interior contradicts to any geological observations. Mantle convection and seemingly chaotic plate movements disqualified any possibilities of earthquake predictions. Earthquakes are triggered during Full or New Moon owing to summarizing action of Moon and Sun torques but relatively scarcely. Mostly, Moon and Sun's torques are subtracted, what decreases probability of

778 earthquakes triggering. Low declinations and from it Moon and Sun low torques also
779 decreases probability of earthquakes triggering. However high tidal torque of Moon,
780 without support of Sun, very often triggers earthquakes. Earthquakes are often
781 triggered by tidal friction, which is manifested by 0º declination because at that time
782 Moon acts along equator. If tidal friction acts before or after Full or New Moon, under
783 such conditions, earthquake occur minimally often without any earthquakes. :
784 Main factor influencing the Earth's behavior is the Earth's rotation axis inclination to
785 the plane of Earth's orbit (obliquity) ±23.5º and also Earth's axis inclination to Moon's
786 plane of orbit varying from ± 28°36′ to ± 18°20′. These values (declination), inserted
787 to formulas (1) and (2) give torques sufficient to move lithospheric plates and by their
788 movement they trigger earthquakes. Let us mention that that Earth's axis is very
789 stable by presence of Moon, as (Laskar et al. 1993) have shown, Moon's variation
790 (nodal cycle) can predict earthquakes (Ostřihanský 2016a,b,c, 2017), Earth's axis
791 wobble the Milankovich cycles (Milankovich 1941) and of course the Earth's axis tilt
792 creates year's seasons.
793 . Considering equilibrium tides, originally developed by Darwin (1879), it assumes
794 that the gravitational potential of the tide raiser can be expressed as the sum of
795 Legendre polynomials P_l. and the shape of a body can be well-represented by a
796 superposition of surface waves with different frequencies and amplitudes.
797 Calculations show semidiurnal uplift of Earth's surface ≈20 cm and related statistics
798 present insignificant results of earthquake triggering with semidiurnal period, (Vidale
799 et al., 1998). Statistics are also disturbed by earthquake delay for several days (in
800 Fig. 13 for 2 days) and cumulative action of tidal friction and north-south tidal torque
801 plus earthquake aftershocks stay earthquakes and their prediction to complicated
802 position.

Mark for conclusion

It is interesting how many incorrect hypotheses has been presented since of 18th century to present. They are for example: Antoniadi's Mars canals/ Volcanic origin of Moon's craters. Neptunists imagination of water effect creating volcanics. Origin of meteorites in atmosphere. Rejecting of plate movements in spite that 1596 Ortelius mentioned continental fit. Wegener's Polflucht, whereas Equator fleeing is correct. Rejecting earthquakes triggering by tides (Vidale, Agnew). Mantle convection driving plates. Mantle plumes originating in mantle-core boundary.

The Earth is not imaginary body but piece of stone heated from inside. Forces moving plates can be imagined by pneumatic hammer mechanism, mantle plumes and subduction by bathyscaphe effect. The Earth originated in melted stage. Consequent solidifying Earth reached the core-mantle boundary. Lithosphere is part of the Earth originally floating on melted Earth. Pressure acting from bottom and sides below lithosphere is equal but pressure acting upwards is lower. Decrease of pressure below lithosphere resulted in decrease of melting temperature and formation of Low velocity zone facilitating the lithospheric plates movement.

Data acquisition

Length of day variations are taken from IERS (Earth rotation service) **http://hpiers.obspm.fr/eop-pc/** Moon and Sun declinations from Sun & Moon position Calculator on Internet, Moon phases from Internet. Earthquakes data for Sumatra, Sulawesi and Italy are taken from ANSS Catalog and EMSC Catalog. For

828 California *A 15 year catalog of more than 1 million low-frequency earthquakes* was
829 taken.
830
831
832

833 Appendix (Calculation of tidal forces)

834 Tidal forces acting on plates are following:
835 1. Forces, which try to align the Earth's flattening to the level of acting tidal forces,
836 i.e. to the planes of Moon and Sun orbits.
837 2. Force, which brakes the Earth's rotation, i.e., the tidal friction.
838
839 **1.** Fig. 1 shows the action of the tidal force in its most effective action during the
840 Sumatra earthquake 2004. The torque acting on the plate can be calculated in
841 following steps (Brož et al 2012):
842 Earth's angular velocity $\omega = 7.29\ 10^{-5}$ rad/sec, Earth's moment of inertia $I = 8.036 \times$
843 10^{37} kg m^2 (Stacey and Davies, 2008). Earth's angular momentum $L = I \times \omega = 5.89$
844 $\times 10^{33}$ kg m^{2}s^{-1}. Mass of the lithospheric bulge is
845

846 $$m_{bulge} = \frac{1}{2}\left(\frac{4}{3}\pi abc - \frac{4}{3}\pi c^3\right)\rho_{crust},$$

847 where we insert $a = b = R_e \approx 6378$ km, $c = R - 21$ km, $\rho_{crust} \approx 2700$ kg m^{-3} and we
848 get $m_{bulge} \approx 9.6 \times 10^{21}$ kg $\approx 1/624\ m_e$. (Earth's mass $m_e = 5.97 \times 10^{24}$ kg). The torque
849 of force couple acting on the Earth is then: in case of the Sun (m_s, r_s Sun's mass and
850 distance, G gravitational constant)

$$M_s = 2 \times \frac{2Gm_{bulge}m_s}{r_s^3} R_e \cos\varepsilon . R_e \sin\varepsilon , \quad (1)$$

where ε = 23.45° is the obliquity of ecliptic to equator. This is valid only in case if the mass of bulge were concentrated in one point on equator and the Sun were just in highest point above equator. In reality we should integrate over the bulge because some its parts are closer to the axis of rotation and to center over the Earth's rotation because the instant angle of the Sun above equator varies. We would get:

$$\overline{M}_s = \frac{1}{4} M_s \approx 5.7 \times 10^{21} \text{ N m}$$

The same calculation is for the Moon:

$$M_m = 2 \times \frac{2Gm_{bulge}m_m}{r_m^3} R_e \cos\iota . R_e \sin\iota , \quad (2)$$

where ι is the Moon's declination (insert 23.45°). The result is $\overline{M}_m = \frac{1}{4} M_m \approx 1.2 \times 10^{22}$ N m. The torques simply summarize $\overline{M} = \overline{M}_s + \overline{M}_m = 1.8 \times 10^{22}$ N m.

This important result calculates that the torque 1.8×10^{22} N m is able to move the plate in north-south direction. The seismic moment of the Sumatra earthquake is 3.5×10^{22} N m (Varga and Denis 2010; Lay et al 2005; Stein and Okal, 2005). Because the torque exerted by tidal force acting on Earth's flattening represents the kinetic energy and also the seismic moment represents energy according to definition $M_0 = \mu AD$, where μ is the shear modulus N/m^2, D is displacement on area A, this quantity of N m dimension represents also energy, both quantities can be compared.

873 **2.** The torques of tidal friction were calculated by Burša (1987a), (1987b) on the
874 basis of angular momentum balance in the Earth – Moon – Sun system.

875 $$N_m = 4.2 \times 10^{35} \text{ kg m}^2 \text{ cy}^{-2} = 4.2 \times 10^{16} \text{ kg m}^2 \text{ s}^{-2} = 4.2 \times 10^{16} \text{ Nm}$$

876 $$N_s = 8.9 \times 10^{34} \text{ kg m}^2 \text{ cy}^{-2} = 8.9 \times 10^{15} \text{ kg m}^2 \text{ s}^{-2} = 8.9 \times 10^{15} \text{ Nm}$$

877 The ratio of tidal torques of Moon and Sun therefore is

878 $$N_m/N_s = 4.7$$

879 According to Jeffreys this ratio is 4.9 (Jeffreys 1975). The Sun's share in tidal friction
880 is only 21%.

881 The tidal fiction decelerates the Earth's rotation (Lambeck, 1977) and therefore it
882 can be also considered as the force causing the westward movement of plates
883 (Ostřihanský 2012a, 2012b Ostřihanský). The torque exerted by the tidal friction is
884 relative low 10^{16} N m. (Burša 1987a) and considering the mantle viscosity only 2
885 orders of magnitude lower than the lithosphere (Cathles 1975), this force is
886 considered as insufficient for the plate movement. But considering variable force (ad
887 1), acting on Earth's flattening, and tidal friction (ad 2) acting semidiurnally, then the
888 westward movement is possible, owing to the north-south varying force ad 1, acting
889 on it perpendicularly.

890

891 **Acknowledgment**

892

893 I would like to express my deep thank to all who dealt with my paper. They are following
894 scientists: Professor Philippe Agard, Professor Carlo Doglioni, Professor Douwe J.J. van
895 Hinsbergen, Dr. Mimmo Palano, Dr. Timothy Horscroft and several others unknown
896 reviewers.

897

898 References

899 Bostrom, R.C., 1971. Westward displacement of the lithosphere. Nature 234, 536 ‐538.

900 Bostrom, R.C., 1973. Arrangement of Convection in the Earth by Lunar Gravity.
901 Philosophical Transactions of the Royal Society of London. Series A, Mathematical and
902 Physical Sciences Vol. 274, No. 1239, 397-407.

903 Brož, M., Solc, M. and Durech, J., 2011. *Physics of small bodies of solar system*, Charles
904 University, Chair of Astronomy, Prague.

905 Broek van den, J.M., Gaina, C., 2020. Microcontinents and continental fragments associated
906 with subduction systems. Tectonics 39, **https://doi.org/10.1029/2020TC006063**.

907 Burša M., 1987a. Secular tidal and non-tidal variations in the Earths rotation. Studia geoph. et
908 geodet. **31,** 219–224.

909 Burša M., 1987b. Secular deceleration of the Moon and of the Earth's rotation in the zonal
910 geopotential harmonics. Bul. Astron Ins. Czechosl, **38**(5), 309-313.

911 Bullard, E. C., 1954. The flow of heat through the floor of the Atlantic Ocean. Proc. Roy. Soc.
912 London A 222, 408–29.

913 Cartwright, D.E., Edden, A., 1973. Corrected Tables of Tidal Harmonics. Geophys. J.
914 Royal Soc. 33, 253 ‐264 .

915 Cathles, L.M., 1975. The Viscosity of the Earth's Mantle. Princeton, Princeton University
916 Press 386 p.

917 Darwin, G. H., 1879. Philosophical Transactions of the Royal Society, **170**, 447, repr.
918 Scientific Papers, Cambridge, Vol. II, 1908 [NASA ADS] [CrossRef] [Google Scholar],

919 Davies, Huw, J., 2013. Global map of solid Earth surface heat flow. Geochem., Geophys.,
920 Geosyst., 14 No.10, 4608-4622, **https://doi.org/10.1002/ggge.20271**.

921 Doglioni, C., 1993. Geological evidence for a global tectonic polarity. J. Geol. Soc. Lond.,
922 150, 991 ‐1002 .

923 Doglioni, C., 1994. Foredeeps versus subduction zones. Geology, 22 (3), 271 ‐274 .

924 Doglioni, C., Panza, G.F., 2015. Polarized plate tectonics. Adv. Geophys., 56 (3), 1 ‑167.
925 https://doi.org/10.1016/bs.agph.2014.12.001 .
926 Doglioni, C., Carminati, E., Bonatti, E., 2003. Rift asymmetry and continental uplift.
927 Tectonics, 22 (3), 1024. https://doi.org/10.1029/2002TC001459 .
928 Doglioni, C., Green, D., Mongelli, F., 2005. On the shallow origin of hotspots and the
929 westward drift of the lithosphere. In: Foulger, G.R., Natland, J.H., Presnall, D.C.,
930 Anderson, D.L. (Eds.), Plates, Plumes and Paradigms. 388. pp. 735 ‑749 Geological
931 Society of America Sp. Paper .
932 Doglioni, C., Carminati, E., Cu _aro, M., Scrocca, D., 2007. Subduction kinematics and
933 dynamic constraints. Earth-Sci. Rev., 83, 125 ‑175 .
934 Doglioni, C., Ismail-Zadeh, A., Panza, G., Riguzzi, F., 2011. Lithosphere-asthenosphere
935 viscosity contrast and decoupling. Phys. Earth Planet. Inter., 189, 1 ‑8.
936 Foulger, G. R., M. J. Pritchard, B. R. Julian, J. R. Evans, R. M. Allen,3 G. Nolet, W. J.
937 Morgan, B. H. Bergsson, P. Erlendsson, S. Jakobsdottir, S. Ragnarsson, R. Stefansson4 K..
938 Vogfjo, R.D., 1971. Seismic tomography shows that upwelling beneath Iceland is confined to
939 the upper mantle. Geophys. J. Int., 146, Issue 2, 504–510 https://doi.org/10.1046/j.0956-
940 540x.2001.01470.x
941 Heezen, B.C., Tharp, M, 1985. In: G. Schoubertand, A. Faure-Moret (Coordinators).
942 Geological World Atlas UNESCO, Paris, 1976, Sheet 18, Antarctic Ocean.
943 Hess, H. H., 1962. History of ocean basins. In Petrologic Studies – A Volume in Honor of A.
944 F. Buddington, pp. 599–620, eds. A. Engeln, H. L. James, & B. F. Leonard. Geol. Soc.
945 America, New York.
946 Holmes, A., 1931. *Radioactivity and Earth Movements*, Trans. Geological Soc., Glasgow, vol
947 18, pp 559–606.

948 Hough, S. E., 2018. Do Large (Magnitude ≥8) Global Earthquakes Occur on Preferred Days
949 of the Calendar Year or Lunar Cycle? Seismol. Res. Lett., January 17, Vol.**89**, 577-581.
950 doi:https://doi.org/10.1785/0220170154,
951 Houtz, R.E., Hayes, D.E., Markl, R.G. 1977. Kerguelen Plateau bathymetry, sediment
952 distribution and crustal structure. Marine Geology 25, 95-99.
953 https://doi.org/10.1016/0025-3227(77)90049-4
954 Jeffreys, H., 1975. The Earth, its Origin, History, and Physical Constitution. Cambridge Univ.
955 Press, Cambridge, England, fourth edition, 420 pp.
956 Jeffreys, H., Crumpin, S., 1970. On the modified Lomnitz law of damping. Mon.Not. R. astr.
957 Soc., 147, 298-301.
958 Kudryavtsev, S., 2004. Improved harmonic development of the Earth tide-generating
959 potential. J. Geod., 77, 829 ‑838.
960 Lambeck, K., 1977. Tidal dissipation in the oceans, astronomical, geophysical and
961 oceanographical consequences. Phil. Trans. Roy. Soc. London. Ser.. A, 287, No. 1347, 545-
962 594.
963 Laskar, J., Joutel F. and Robutel, P. 1993. Stabilization of the Earth's obliquity by the Moon.
964 Nature, 361, 615 [NASA ADS] [CrossRef] [Google Scholar]
965 Lay, T., H. Kanamori, C. J. Ammon, M. Nettles, S. N. Ward, R. C. Aster, S. L. Beck, S. L.
966 Bilek, M. R. Brudzinski, R. Butler, H. R. Deshon, G. Ekstrom, K. Satake, and Sipkin, S.
967 2005. The great Sumatra-Andaman earthquake of 26. December 2004, Science, **308**, 1127–
968 1132.
969 Métivier, L., de Viron, O., Conrad, C. P., Renault, S., Diament, M., & Patau, G., 2009.
970 Evidence of earthquake triggering by the solid earth tides. Earth Pl. Sci. Lett., 278, 370–37.
971 Minster, J.R., Jordan, T.H., 1978. Present-day plate motions. J.Geophys Res., 83, 5331-5254.

Milanković, M. 1941. Kanon der Erdbestrahlung und seine Anwendung auf das Eiszeitenproblem., Königliche Serbische Akademie, XX, 633.

Moore, G.W., 1973. Westward tidal lag as the driving force of plate tectonics. Geology, 1, 99‑100. https://doi.org/10.1130/0091-7613.

Ostřihanský, L., 1978. The radioactivity of the Earth's crust in the area of crystalline rocks in Bohemian Massif and its influence on the terrestrial heat flow. (in Czech with English abstract), Geophysical Institute of Czechoslovak Academy of Science, Prague.

Ostřihanský, L., 1980. The structure of the Earth's crust ant the heat flow – heat generation relationship in the Bohemian Massif. Tectonophysics 68, 325-337.

Ostřihanský, L., 1997. The causes of lithospheric plates movements, Charles University Prague, Chair of Geography and Geoecology, 64 pp.

Ostřihanský, L., 2012a. Earth's rotation variations and earthquakes of 2010-2011, Solid Earth Discuss., **4**, 33-130, doi.org/10.5194/sed-4-33-2012,.

Ostřihanský, L.,, 2012b. Causes of earthquakes and lithospheric plates movement, Solid Earth Discuss., **4**, 1411–1483, doi:10.5194/sed-4-1411-2012.

Ostřihanský, L,. 2015. Tides as drivers of plates and criticism of mantle convection, Acta Geod. Geophys., (3), 271-293, doi: 10.1007/s40328-014-0080-6.

Ostřihanský, L., 2016a. The correct mechanism of lithospheric plates movement, Poster at Session: Plate motion, Continental Deformation and Intraseismic Strain Accumulation, AGU Fall Meeting 2016, San Francisco 12-16 December 2016.

Ostřihanský, L., 2016b. Verification of tidal earthquake triggering in Central Italy, Poster at Session: The 24 August 2016 Earthquake, AGU Fall Meeting 2016, San Francisco 12-19 December 2016.

Ostřihanský, L., 2016c. The next strong earthquake in Central Italy will be in autumn 2034, Available on ResearchGate.

997 Ostřihanský, L, 2017a. The next strong earthquake in South-Central Alaska will be in 2021,
998 Project Earthquake prediction. June 2017, doi**:** 10.13140/RG.2.2.18897.94569**.**
999 Ostřihanský, L., 2017b. Fortnightly dependence of San Andreas tremor and low frequency
1000 earthquakes on astronomical parameters, Available on ResearchGate,.
1001 Ostřihanský, L., 2019a. Tides as triggers of earthquakes in Sulawesi (Completed). Available
1002 on ResearchGate.
1003 Ostřihanský, L., 2019b. Summary of the most evident tidal actions on solid Earth. Available
1004 on ResearchGate.
1005 Ostřihanský, L., 2020. Principles of lithospheric plates movements and earthquakes
1006 triggering. Available on ResearchGate.
1007 Riguzzi F., Panza G., Varga P. and Doglioni C., 2009. Can Earth's rotation and tidal
1008 despinning drive plate tectonics? Tectonophysics, 484, 60-73,
1009 Revelle, R., Maxwell, A.E., 1952. Heat flow through the floor of the eastern North Pacific
1010 Ocean. Nature, 170, 199–200.
1011 Schmucker, U., 1969. Geophysical aspects of structure and composition of the Earth, in
1012 Handbook of Geochemistry, Vol. I (ed. K. H. Wedepohl). Berlin. Springer-Verlag, pp. 134–
1013 226.
1014 Schubert, G., Garfunkel, Z., 1984. Mantle upwelling in the Dead Sea and Salton Trough-
1015 Gulf of California leaky transforms. Ann. Geophysicae, 2, 633–48.
1016 Schubert, G., Turkotte. D.L., Olson, P., 2004. Mantle convection in Earth and planets.
1017 Cambridge University Press, 2004.
1018 Shelly, D.R, 2017. A 15 year catalog of more than 1 million low-frequency earthquakes:
1019 Tracking tremor and slip along the deep San Andreas Fault. US Geol Survey DOI:
1020 10.1002/2017JB014047, 2017.

1021 Stacey, F.D., and Denis, P.M., 2008. *Physics of the Earth*, Cambridge University Press, 544
1022 pp.
1023 Stein, S. and Okal, E.A., 2005. Size and speed of the Sumatra earthquake, Nature 434, 581-
1024 582.
1025 Takahashi, E., Kushiro, I., 1983. Melting of a dry peridotite at high pressures and basalt
1026 magma genesis. Am. Mineral., 68, 859–79.
1027 Tanaka, S., 2010. Tidal triggering of earthquakes precursory to the recent Sumatra megathrust
1028 earthquakes of 26 December 2004 (Mw 9.0), 28 March 2005 (Mw 8.6), and 12 September
1029 2007 (Mw 8.5). Geophys. Res. Lett., 37, L02301. doi: 10.1029/
1030 2009GL041581.
1031 Tanaka, S., 2012. Tidal triggering of earthquake prior to the 2011 Tohoku-Oki artquake
1032 (MW9.1). Geophys. Res. Lett., 39, L00G26. doi: 10.1029/2012GL051179.
1033 Van der Elst, N.J., Delorey, A.A., Shelly, D.R., Johnson, P.A., 2016. Fortnightly modulation
1034 of San Andreas tremor and low-frequency earthquakes. PNAS 113 (31), 8601-8605.
1035 van Hinsbergen, D J. J., Lippert, P.C., Dupont-Nivet, G., McQuarrie, N., Doubrovine, P.V.,
1036 Spakman, W/ and Torsvik., T. H., 2012. Greater India Basin hypothesis and a two-stage
1037 Cenozoic collision between India and Asia. PNAS 109 (20) 7659-
1038 7664; https://doi.org/10.1073/pnas.1117262109
1039 Varga, P and Denis, C., 2010.Geodetic aspect of seismological phenomena, Journal of
1040 Geodesy, **84**, 107-121, doi.org/10.1007/s00190-009-0350-1.
1041 Varga, P. and Grafarend, E., 2017. Influence of Tidal Forces on the Triggering of Seismic
1042 Event, Pure Appl. Geophys., **175**, 1649-1657. doi.org/10.1007/s00024-017-1563-5.
1043 Vidale, J. E., Agnew, D. C., Johnston, M. J. S., and Oppenheimer, D. H., 1998. Absence of
1044 earthquake correlation with Earth tides: An indication of high preseismic fault stress rate. J.
1045 Geophys. Res. B Solid Earth, **103**, 24567–24572.

1046 Vink, G.E., Morgan, J.W., Zhao, W.L., 1984. Preferential rifting of continents: A source of
1047 displaced terranes. J.Geophys.Res., 89, No B 12, 10072-10074.
1048 Wegener, A., 1929. Die Enstehung der Kontinente und Ozeane. Vieweg, Braunschweig,
1049 fourth edition.
1050 Yoder, C.F., Williams, J.G., Paeke, M.E., 1981. Tidal variations of Earth rotation. J. Geophys
1051 Res, No B2, 881-891.
1052 Zaccagnino, D., Vespe, F., Doglioni, C., 2020. Tidal modulation of plate motions. Earth
1053 Science Reviews. https://doi.org/10.1016/j.earscirev.2020.103179. Journal homepage:
1054 www.elsevier.com/locate/earscirev.
1055
1056
1057
1058